

SNX

Swiss-Norwegian Foundation for Research with X-Rays

Annual Report 2023

Contents

General Remarks.....	5
Introduction	6
ESRF highlights from SNBL	7
Making bilayer LLZO membranes for solid-state batteries: exploring the sintering process with X-ray diffraction.....	8
Pyrochlore iron hydroxy fluorides: Affordable lithium-ion cathode materials for stationary energy storage	11
Unravelling the complexity of magnesium borohydride-ethylenediamine solid-state electrolytes.....	14
X-rays reveal challenges in scaling up a catalyst for CO ₂ hydrogenation to propane	17
SNBL's Outreach.....	19
Tech talk article on the ESRF frontpage.....	19
ESRF and long standing SNBL user awarded 2023 Bragg prize	22
ESRF news December 2023.....	23
Swiss Summer School on Diffraction and Crystallography, BM01-ESRF.....	24
SNBL publications on journal covers.....	26
Involvement of SNBL in ESRF STREAMLINE cross-cut review	30
Development of enabling technologies	31
BM01 SAXS/WAXS design and procurement.....	31
Software developments.....	32
Sample environment development program	32
XAFS-XRD Catalysis high temperature and pressure micro flow reactor	32
1 st XRD Ultra-fast high temperature heater 1100°C	33
2 nd XRD Ultra-fast high temperature heater 1300°C (NTNU – ELKEM – SNBL).....	34
Total Scattering operando liquid electrolyte battery cell (Uni Oslo – SNBL).....	34
XAFS-XRD operando Solid State Battery cell (NTNU – SNBL).....	35
EXAFS/XRD/PDF operando electrochemistry cell (Uni Bern – SNBL).....	36
XRD 1000 Bar Sapphire Capillary Cell.....	37
References related to sample environment developments	38
Scientific output Impact Factors	39
Scientific output Research Areas	40
Involvement of industry in SNBL's publication output	41
Publication list 2023.....	44

General Remarks

The year 2023 is the twentieth year of the SNX Foundation.

The accounting is supervised by OPTIMA COMPTA, in Seyssinet-Pariset, in Isère, for the two French associations, and by BfB Fidam Fiduciaire in Renens VD for the SNX Foundation. AUDICT FIDUCIAIRE in Lausanne audits the accounts.

These legal frameworks contribute to the smooth running of the collaborations and to the successful scientific work done at the Swiss Norwegian Beam Lines at ESRF.

The activities of the SNX Foundation are carried out at the European Synchrotron Radiation Facility (ESRF) in Grenoble and comprise the operation and up-grade of two beam line branches, called the Swiss-Norwegian Beam Lines (SNBL).

Introduction

This report covers the year 2023, the third of the 4-year contract (2021-2024) between the Swiss partner, the École Polytechnique Fédérale de Lausanne (EPFL) and for Norway the Norwegian University of Science and Technology (NTNU).

Obviously, the user program continued in 2023, moreover the major upgrade program, spanning over the 4-year contract period, is starting to impact the scientific output. This plan foresees that on BM01, Bragg diffraction, diffuse and small angle scattering, for single crystal, thin films and powder samples will become available. On BM31 the combined diffraction and X-ray absorption experiments setup is completed with Total Scattering and improvements in time and space resolution for all techniques. The BM01 phase 2 upgrade has moderate cost. The BM31 phase 2 project however has a total investment budget of ~2 Million Euro's. Where 2021 was very much a development and investment year. 2022 was marked by a massive assembly, testing, installation and implementation works on especially the BM31 beamline while running practically a full user program. On BM31, 2023 has been devoted to, on the one hand, help the user community in making use of the new capabilities. While on the other hand, the sample environment for both stations was developed intensively in order to match with the new opportunities. On BM01, the SAXS/WAXS setup has moreover been designed and acquired in 2023. On both beamlines much effort has also been put in streamlining the operation by further developing and implementing new software tools. Overall the works and output can be summarized as follows:

1. The user program was successfully and reliably executed on both beamlines.
2. 67 publications using SNBL data appeared in peer review journals, 30% of SNBL publications has an impact factor above 10 and 80% above impact factor 4.
3. On BM01 the SAXS/WAXS setup was designed and acquired.
4. An intense sample environment development program was initiated resulting in the employment of seven state of the art devices.

ESRF highlights from SNBL



ESRF HIGHLIGHTS 2023



Making bilayer LLZO membranes for solid-state batteries: exploring the sintering process with X-ray diffraction

Dense–porous bilayer membranes were manufactured as a separator for high-performance lithium-garnet solid-state batteries. *In-situ* X-ray diffraction revealed the chemical reactions that occur during high-temperature sintering, emphasising the importance of the sintering step in manufacturing solid-state electrolytes.

In battery research, the replacement of liquid lithium (Li)-ion electrolytes with their non-flammable and non-toxic solid counterparts based on $\text{Li}_7\text{La}_3\text{Zr}_2\text{O}_{12}$ (LLZO) with the garnet-type structure is pursued as a compelling approach to improve the energy density, cycling stability and safety of Li-ion batteries [1]. However, commercial Li-garnet solid-state batteries still face performance challenges, especially with the Li/LLZO interface, leading to low cycling stability and Li dendrite formation (projections of metal that can build up on the lithium surface and penetrate into the solid electrolyte, eventually crossing from one electrode to the other and shorting the battery cell). To address Li dendrite formation, an innovative dense–porous LLZO microstructure design has been proposed [2]. It offers solutions to mitigate dendrite-related issues by enabling Li storage in the scaffold during deposition, reducing volume changes and minimising void formation. Additionally, a denser layer can act as a protective barrier against Li dendrites.

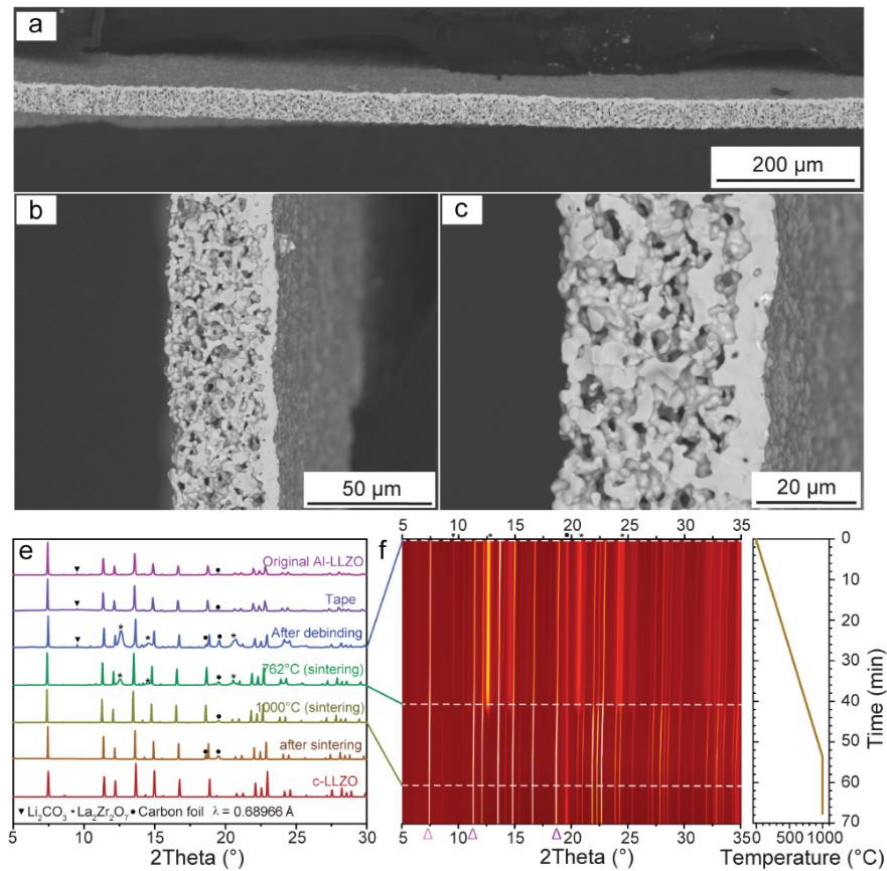


Fig. 1: a-c) Cross-section SEM images of LLZO membranes after sintering. e) XRD patterns of LLZO membrane at different stages during manufacturing process. f) Measured XRD map of LLZO membrane during sintering. Right side: Temperature profile of the heat-treatment.

This work introduces an innovative tape-casting technique for LLZO membrane manufacture, involving the sequential casting of dense (8-10 μm) and porous (32-35 μm) layers. In short, bilayer dense–porous LLZO membranes were prepared via the following steps: i) Preparation of slurries for porous and dense LLZO layers, ii) their sequential tape-casting, iii) pilling off the LLZO tape from the substrate, iv) de-binding, and v) sintering. As shown in Figure 1a-c, no delamination was observed between the two layers along the entire interface of the prepared membranes after sintering, showing good adhesion between the two layers. X-ray tomography images showed that the porous layer contained only open-pore channels with a porosity above 50 vol%, while the dense layer showed no porosity, was pinhole-free and had a continuous dense structure.

Preliminary experiments revealed that the addition of Li_2CO_3 as an additive to compensate Li-losses during de-binding and sintering is paramount for obtaining an impurity-free cubic LLZO phase. Thus, it was identified that in the case of using LLZO powder without the addition of Li_2CO_3 , the sintered LLZO membranes contained large quantities of $\text{La}_2\text{Zr}_2\text{O}_7$ (LZO). To understand the chemical transformations that occur during de-binding and sintering of tape-casted LLZO tapes, the tapes were analysed by *in-situ* synchrotron X-ray diffraction (XRD) at beamline **BM01**. The experiments revealed that multiple chemical processes occur (Figure 1e-f). First, the de-binding causes the formation of a relatively large quantity of the LZO phase, as follows from the comparison of as-prepared LLZO tape and de-binded LLZO membranes. Upon a further increase of temperature to 760°C, however, the intensity of LZO reflections starts to disappear, resulting in the formation of a solely cubic LLZO structure. This process is accompanied by the disappearance of the Li_2CO_3 peak at $\approx 716^\circ\text{C}$, which is likely associated with the melting of Li_2CO_3 , decomposition to Li_2O and following reaction with LZO. Importantly, membranes with higher Li_2CO_3 content were observed to have higher density. This observation is in line with the reported impact of Li_2CO_3 on the densification of LLZO pellets. It is assumed that this effect is related to the melting of Li_2CO_3 , which allows to initiate the sintering process at lower temperatures. LLZO ceramics without additional Li_2CO_3 require a higher temperature and longer time for sintering, potentially causing huge Li-loss.

After extra-thermal surface treatments to clean the impurities on the LLZO membrane, the electrochemical functionality of the developed bi-layered dense–porous LLZO scaffolds was investigated in full hybrid-type cells in combination with a paste-type lithium ion phosphate (LFP) cathode (as a proof-of-concept battery in Figure 2a-b). Figure 2c-d shows the voltage profiles and cycling stability measurements of an LFP/LLZO/Li full cell measured at 0.1 C rate. The cell delivered the capacity of LFP of $\approx 100\text{-}150 \text{ mAh g}^{-1}$, which corresponds to the areal capacity of $\approx 0.3\text{-}0.45 \text{ mAh cm}^{-2}$. The results demonstrate a relatively low capacity retention of 65% after 30 cycles. Besides, in symmetrical cell configuration, the LLZO membranes exhibit a high critical current density (6 mA cm^{-2}), low overpotentials ($14\text{-}16 \text{ mV}$ at 1.0 mA cm^{-2}), and excellent Li plating/stripping cycling stability (over 160 cycles at 0.5 mA cm^{-2} with a 0.25 mAh cm^{-2} areal capacity limitation).

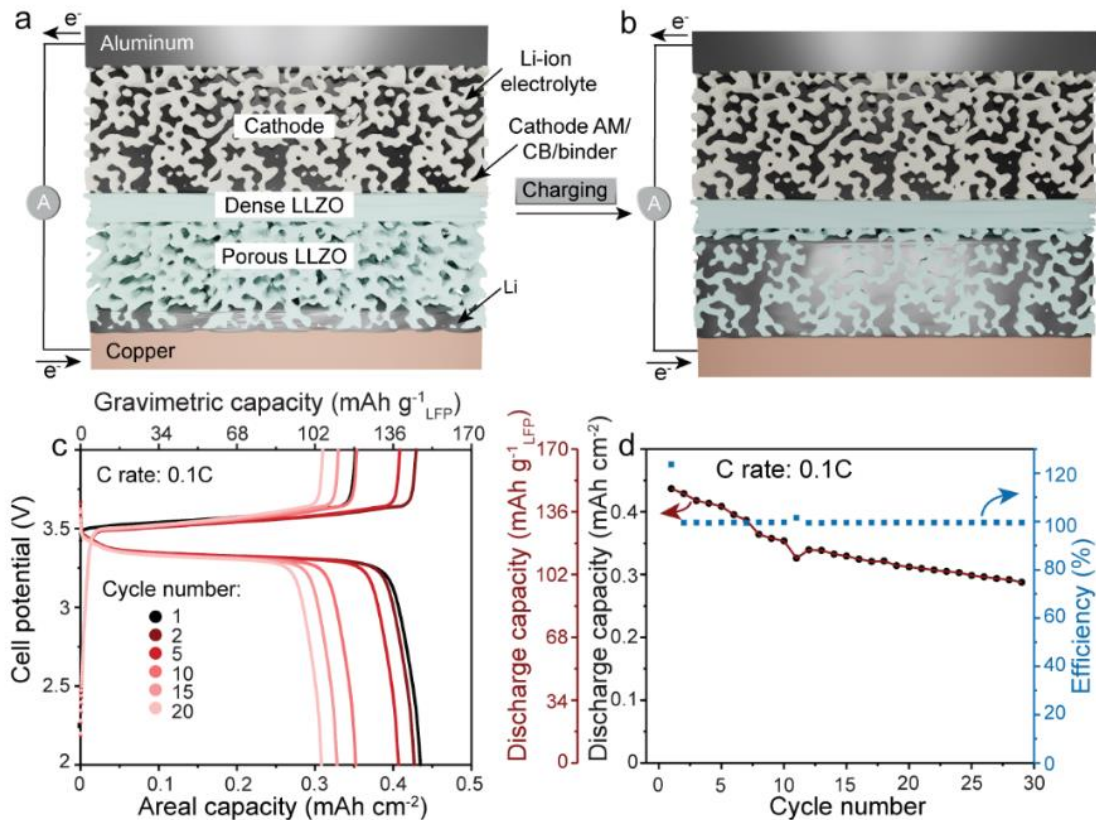


Fig. 2: a-b) Schematics of the charging process of Li-garnet solid-state batteries based on dense-porous LLZO membrane. Galvanostatic charge-discharge (c) voltage profiles and (d) cyclic stability of LFP/LLZO membrane/Li full cells measured at 0.1 C rate and room temperature without the employment of external pressure.

In summary, this work reports a methodology for manufacturing dense-porous LLZO membranes with thicknesses maximally close to those required for achieving high gravimetric and volumetric energy densities of Li-garnet solid-state batteries, and contributes to enabling their eventual commercialisation.

Principal publication and authors

Bilayer Dense-Porous $\text{Li}_7\text{La}_3\text{Zr}_2\text{O}_{12}$ Membranes for High-Performance Li-Garnet Solid-State Batteries, H. Zhang (a,b), F. Okur (a,b), C. Cancellieri (c), L.P.H. Jeurgens (c), A. Parrilli (d), D.T. Karabay (a,b), M. Nesvadba (a,b), S. Hwang (a,b), A. Neels (d), M.V. Kovalenko (a,b), K.V. Kravchyk (a,b), *Adv. Sci.* 8, 2205821 (2023); <https://doi.org/10.1002/advs.202205821>

(a) Department of Chemistry and Applied Biosciences, ETH Zürich, Zürich (Switzerland)

(b) Laboratory for Thin Films and Photovoltaics, Empa, Dübendorf (Switzerland)

(c) Laboratory for Joining Technologies & Corrosion, Empa, Dübendorf (Switzerland)

(d) Center for X-Ray Analytics, Empa, Dübendorf (Switzerland)

References

[1] K.V. Kravchyk *et al.*, *Sci. Rep.* 12, 1177 (2022).

[2] K. Fu *et al.*, *Energy Environ. Sci.* 10, 1568-1575 (2017).

Pyrochlore iron hydroxy fluorides: Affordable lithium-ion cathode materials for stationary energy storage

A new, cost-effective synthesis method for pyrochlore iron (III) hydroxy fluorides (Pyr-IHF) for economical stationary-energy-storage materials demonstrates high capacity retention over 600 cycles without complex electrode design. *Operando* X-ray diffraction was used to investigate water crystallisation and its effect on electrochemical performance in Pyr-IHF.

The shift from fossil fuels to renewable energy sources necessitates cost-effective stationary rechargeable batteries for energy balance. Iron (III) fluoride-based compounds are being explored as economical lithium-ion battery cathodes due to their abundant constituents and high capacity [1]. Pyrochlore iron (III) fluorides (Pyr-FeF₃) with large hexagonal channels show promise for enhanced Li-ion diffusion [2]. However, a cost-effective Pyr-FeF₃ synthesis method has been elusive. In this study, a straightforward, ambient-condition synthesis method was developed for Pyr-IHF from an ethanol-dissolved precursor, achieving over 80% capacity retention after 600 cycles. Investigation of water content within Pyr IHF channels confirmed its impact on capacity and Li-ion diffusion. This research advances low-cost materials for renewable energy integration.

The synthesis of Pyr-IHF involved dissolving FeF₃(H₂O)₂ · H₂O in ethanol, followed by water-induced precipitation. The as-synthesised Pyr-IHF consisted of size-uniform spherical nanoparticles with a cubic pyrochlore structure, featuring 3D interconnected hexagonal channels. Wavelet-transformed extended X-ray absorption fine structure (EXAFS) analysis, obtained at beamline BM31, was used in combination with infrared spectroscopy to determine an average coordination environment of FeF₄(OH)₂ octahedra. Rietveld refinement of synchrotron X-ray diffraction (XRD) performed at beamline BM01 indicated the presence of water of crystallisation in the Pyr-IHF structure, contributing to larger lattice parameters and suggesting a chemical formula of FeF₂(OH) · 0.7 H₂O for as-synthesized Pyr-IHF.

The structural changes during heat-treatment of as-synthesised Pyr-IHF were analysed using *operando* XRD obtained at beamline **BM01** (Figure 1). The analysis revealed two distinct stages of lattice parameter contraction during heating, with the first contraction occurring between 75-125°C and the second between 220-280°C. The initial contraction was attributed to the release of disordered water molecules from within the channels. The second unit cell contraction was linked to the release of the water of crystallisation, confirmed by changes in the occupancy of crystalline water. In the presence of residual moisture, Pyr-IHF could be partially rehydrated during cooling. The appearance of small-angle X-ray scattering (SAXS) signals indicated morphological changes in Pyr-IHF particles during the release of disordered water within the channels, which was further confirmed by transmission electron microscopy (TEM). Furthermore, despite a loss in crystallinity during heat-treatment, Pyr-IHF retained its local structure, as confirmed by X-ray absorption spectroscopy (XAS) obtained on **BM31** showing highly similar features in the spectra before and after heat-treatment.

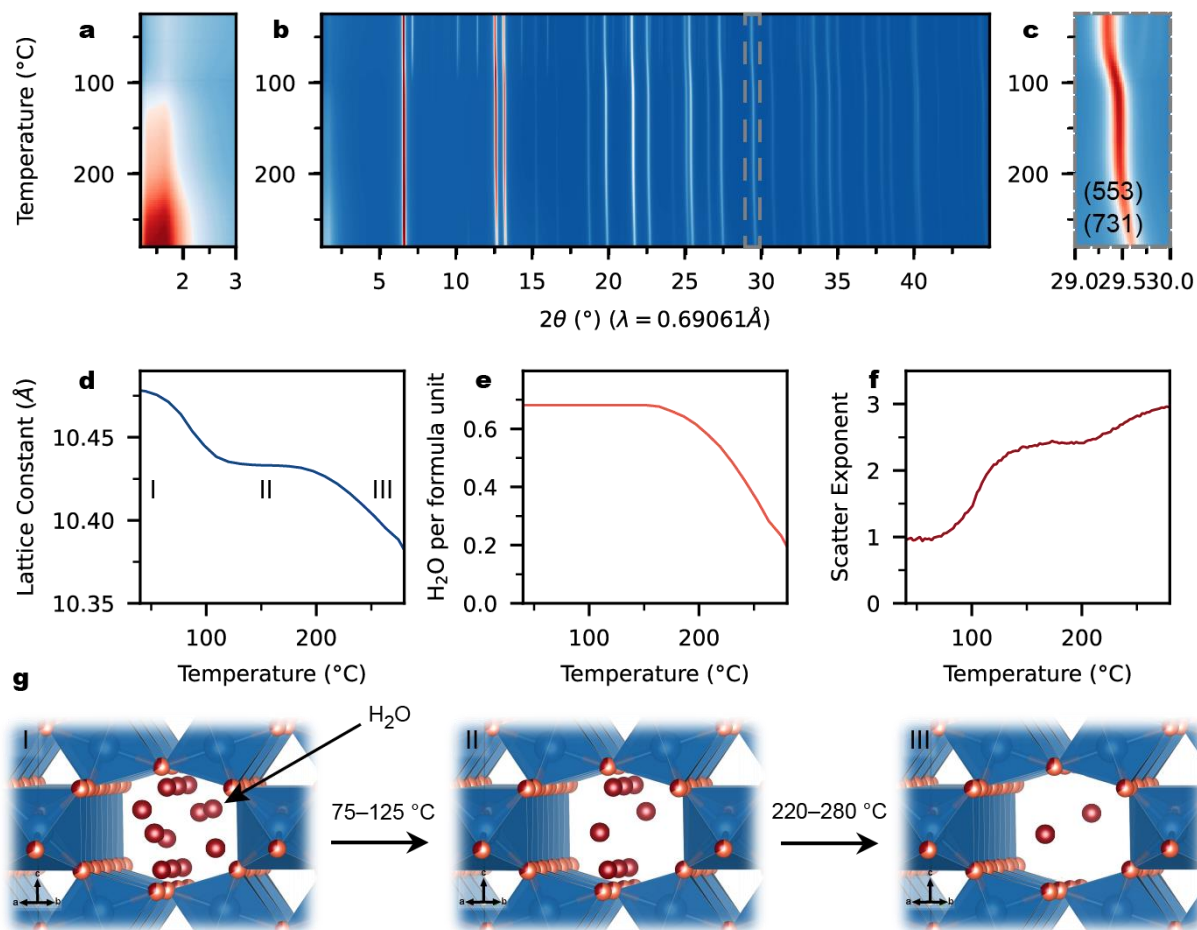


Fig. 1: Structural changes in Pyr-IHF during heat-treatment. a-c) *Operando* XRD of the heat-treatment of as-synthesised Pyr-IHF. d,e) Temperature evolution of Pyr-IHF lattice constant (d), crystalline water content inside the channels (e). f) Fitted scattering exponent obtained from SAXS. g) Schematic representation of the H₂O loss in Pyr-IHF during heat-treatment.

Finally, the impact of structural water on the electrochemical performance of Pyr-IHF was studied by preparing a series of cathodes with varying water content and cycling them at different current rates (Figure 2). Pyr-IHF samples with similar porosities with less water content exhibited significantly higher capacities, indicating that the presence of water inside the Pyr-IHF channels negatively affected both Li-ion storage and diffusion, reminiscent of an intercalation-type mechanism for Li-ion storage.

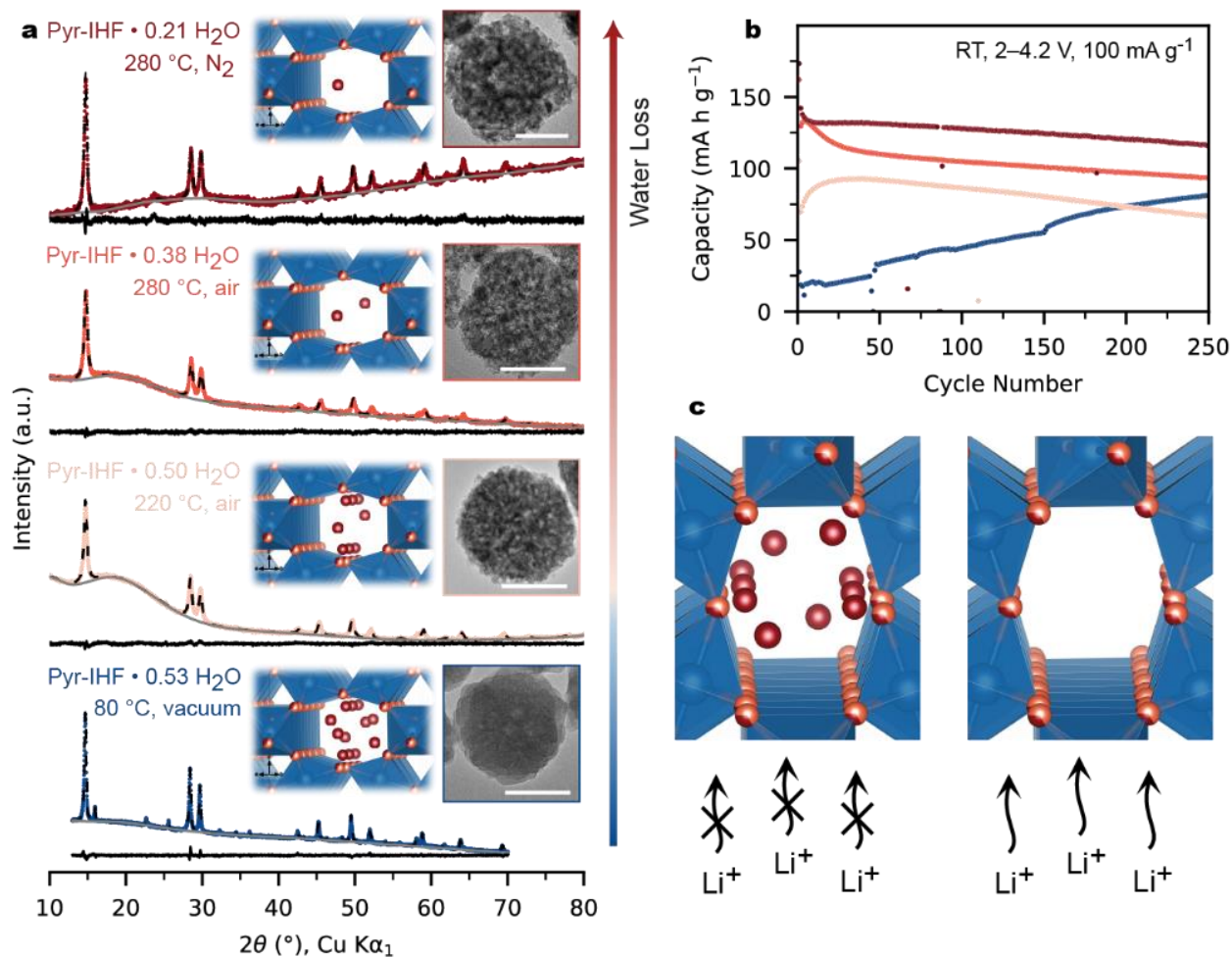


Fig. 2: Influence of morphology and water of crystallisation on the electrochemical performance of Pyr-IHF Cathodes. a) Rietveld refinements and TEM micrographs (100 nm scale bars) for the Pyr-IHF samples of different crystalline H₂O content. b) Cycling stability of the same Pyr-IHF cathodes. c) Schematic representation of the effect of H₂O inside the channels of Pyr-IHF on the Li-ion storage ability.

In summary, this study presents a cost-effective and scalable synthesis of Pyr-IHF with well-defined morphology and narrow particle size distribution. The dissolution-precipitation process enhances Li-ion conducting channels from 1D to 3D. Heat-treatment selectively modifies the morphology and solvent content within the 3D channels. *Operando* XRD measurements revealed that changes in surface morphology are linked to the removal of solvent molecules from the Pyr-IHF crystal structure during heating. Batteries with heat-treated Pyr-IHF cathodes exhibited exceptional cycling stability, showcasing its potential as a low-cost cathode material. Additionally, removing water of crystallisation from the channels significantly improves capacity, highlighting the role of Pyr-IHF's channels in facilitating Li-ion diffusion. This work provides the first evidence of Li-ion intercalation behaviour in Pyr-IHF, warranting further investigation into structural changes during Li-ion intercalation.

Principal publication and authors

Pyrochlore Type Iron Hydroxy Fluorides as Low-Cost Lithium-Ion Cathode Materials for Stationary Energy Storage, J.F. Baumgärtner (a,b), M. Wörle (a), C.P. Guntlin (a), F. Krumeich (a), S. Siegrist (a), V. Vogt (a), D.C. Stoian (c), D. Chernyshov (c), W. van Beek (c), K.V. Kravchyk (a,b), M.V. Kovalenko (a,b), *Adv. Mater.* 2304158 (2023); <https://doi.org/10.1002/adma.202304158>

(a) *Laboratory of Inorganic Chemistry, Department of Chemistry and Applied Biosciences, ETH Zürich, Zürich (Switzerland)*

(b) *Laboratory for Thin Films and Photovoltaics, Empa – Swiss Federal Laboratories for Materials Science and Technology, Dübendorf (Switzerland)*

(c) *Swiss–Norwegian beamlines, ESRF*

References

[1] F. Wu, G. Yushin, *Energy Environ. Sci.* 10, 435 (2017).

[2] C. Li *et al.*, *J. Am. Chem. Soc.* 135, 11425 (2013).

Unravelling the complexity of magnesium borohydride-ethylenediamine solid-state electrolytes

By combining synchrotron X-ray and neutron diffraction experiments, the intricate architecture of a solid-state electrolyte made from magnesium borohydride and ethylenediamine has been unravelled. The structural complexity offers valuable insights into enhancing magnesium-ion battery technology.

Magnesium-ion batteries (MIBs) are emerging as a promising alternative to traditional lithium-ion batteries due to their higher energy density and the abundance of magnesium in the Earth's crust [1]. The key to realising the full potential of MIBs lies in developing efficient solid-state electrolytes that facilitate the transport of magnesium ions within the battery. Single-crystal X-ray diffraction at beamline **BM01** and neutron powder diffraction at J-PARC proton accelerator, Japan, were used to unveil the structural intricacies of the magnesium borohydride-ethylenediamine system, a promising candidate solid-state electrolyte for MIBs.

Annealing of a ball-milled sample made it possible to grow single crystals of about 20 μm , suitable for structure determination using synchrotron X-ray diffraction. The structure of the conductive compound (Figure 1), initially believed to be $\text{Mg}(\text{en})_1(\text{BH}_4)_2$ [2], was revealed to be far more complex than originally thought. Contrary to the initial assumption, it was determined to be $\text{Mg}_5(\text{en})_6(\text{BH}_4)_{10}$, indicating a 5:6 stoichiometric ratio of magnesium to ethylenediamine. Magnesium atoms exhibited three different coordination numbers: 4, 5, and 6. This variation in coordination numbers confirms the diverse roles of the ligands in the structure: ethylenediamine plays a dual role as both a chelating and bridging ligand in the cation and anion; borohydride ions (BH_4^-) serve as terminal and bridging ligands, contributing to the compound's structural complexity.

Remarkably, the structure of $\text{Mg}_5(\text{en})_6(\text{BH}_4)_{10}$ is not densely packed, revealing the presence of small voids that occupy nearly 3% of the structure volume. These voids could potentially play a crucial role in facilitating magnesium ion mobility within the solid-state electrolyte. These newly evidenced structural features open new avenues for understanding the mechanism of magnesium ion diffusion in solid-state electrolytes, a crucial factor for MIB performance.

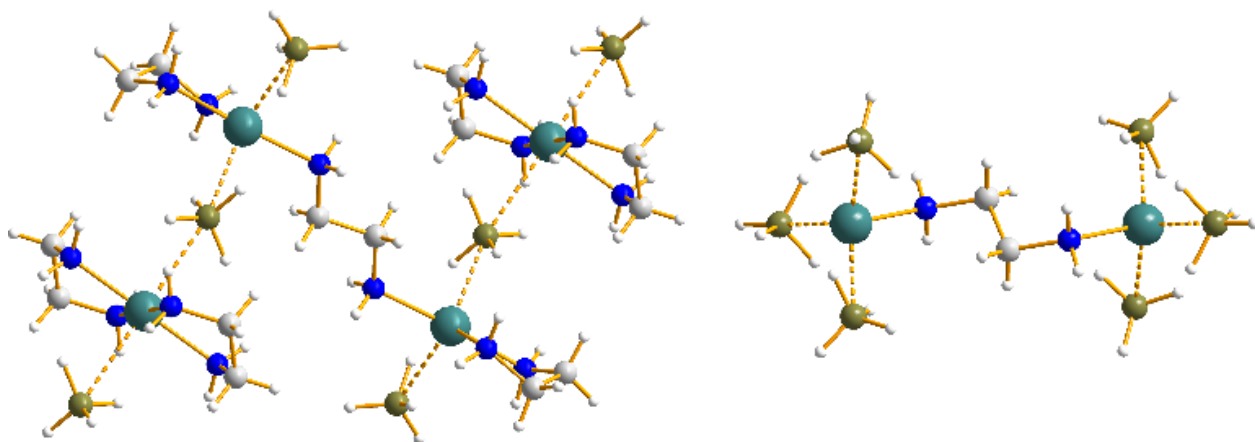


Fig. 1: Crystal structure of $\text{Mg}(\text{en})_{1.2}(\text{BH}_4)_2$: the isolated binuclear anion $[\{\text{Mg}(\kappa^3\text{-BH}_4)(\kappa^2\text{-BH}_4)_2\}_2(\mu_2\text{-en})]^{2-}$ is represented on the right and the $[\text{Mg}_3(\text{en})_5(\text{BH}_4)_4]^{2+}$ cation constituting the coordination polymer chains, $[\text{Mg}^{2+}(\kappa^2\text{-en})_2(\mu_2, \kappa^{1,2}:\kappa^2\text{-BH}_4^-)\text{Mg}^{2+}(\kappa^2\text{-en})(\kappa^2\text{-BH}_4^-)(\mu_2\text{-en})\text{Mg}^{2+}(\kappa^2\text{-en})(\kappa^2\text{-BH}_4^-)(\mu_2, \kappa^2:\kappa^{1,2}\text{-BH}_4^-)]$, on the left. Colour code: Mg - aquamarine, N - blue, B - olive, C - grey, H - white.

Furthermore, variable-temperature X-ray powder diffraction complemented by density functional theory (DFT) optimisation revealed that $\text{Mg}_5(\text{en})_6(\text{BH}_4)_{10}$ transforms into another phase upon heating, with a stoichiometry hitherto unobserved within the magnesium borohydride-ethylenediamine system – $\text{Mg}(\text{en})_2(\text{BH}_4)_2$ (Figure 2). The data suggest that the formation of the crystalline $\text{Mg}(\text{en})_2(\text{BH}_4)_2$ is accompanied by the formation of amorphous $\text{Mg}(\text{BH}_4)_2$. The amorphous phase also forms upon mechano-chemical synthesis, decreasing the conductivity of the samples, but it is omitted in the phase analysis made by X-ray diffraction.

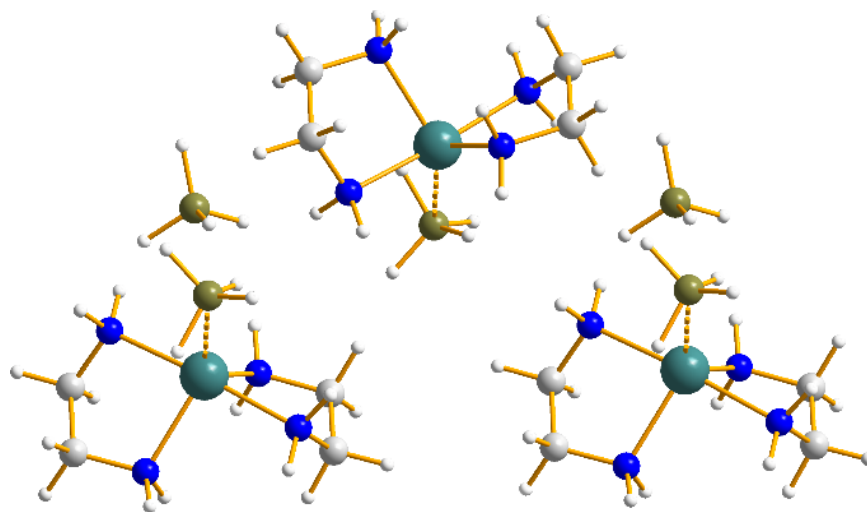


Fig. 2: Fragment of the crystal structure of $\text{Mg}(\text{en})_2(\text{BH}_4)_2$. Colour code: Mg - aquamarine, N - blue, B - olive, C - grey, H - white.

In summary, new insights into the structural complexity of the magnesium borohydride-ethylenediamine solid-state electrolyte system were obtained through synchrotron X-ray and neutron diffraction. The existence of $\text{Mg}_5(\text{en})_6(\text{BH}_4)_{10}$ and $\text{Mg}(\text{en})_2(\text{BH}_4)_2$, which results from thermal decomposition of the former, were evidenced for the first time. The surprising voids observed in the structure of $\text{Mg}_5(\text{en})_6(\text{BH}_4)_{10}$ might be

fundamental to its conductivity. The results of this study, including comprehending the role of the amorphous $\text{Mg}(\text{BH}_4)_2$, are key to the further understanding and enhancement of solid-state electrolytes for MIBs.

Principal publication and authors

Structural insight into the magnesium borohydride-ethylenediamine solid-state Mg-ion electrolyte system, I.E. Golub (a), M. Heere (b,c), V. Gounaris (a), X. Li (a), T. Steenhaut (a), J. Wang (a), K. Robeyns (a), H.-W. Li (d), I. Dovgaliuk (e,f), K. Ikeda (g), G. Hautier (a), Y. Filinchuk (a), *Dalton Trans.* 52(8), 2404-2411 (2023); <https://doi.org/10.1039/D2DT03567G>

(a) *Institute of Condensed Matter and Nanosciences (IMCN), Université catholique de Louvain (UCLouvain), Louvain-la-Neuve (Belgium)*

(b) *Institute for Applied Materials—Energy Storage Systems (IAM-ESS), Karlsruhe Institute of Technology (KIT), Eggenstein (Germany)*

(c) *Technische Universität Braunschweig, Institute of Internal Combustion Engines, Braunschweig (Germany)*

(d) *Hefei General Machinery Research Institute (HGMRI), Hefei (China)*

(e) *Swiss–Norwegian Beamlines, ESRF, Grenoble (France)*

(f) *Institut des Matériaux Poreux de Paris, Ecole Normale Supérieure, Paris (France)*

(g) *Institute of Materials Structure Science, High Energy Accelerator Research Organization (KEK), Tsukuba (Japan)*

References

[1] S. Payandeh, A. Remhof & C. Battaglia, in *Magnesium Batteries: Research and Applications*, Maximilian Fichtner (ed.), The Royal Society of Chemistry (Cambridge, UK), 60-78 (2020).

[2] E. Roedern *et al.*, *Sci. Rep.* 7, 46189 (2017).

[3] O.A. Babanova *et al.*, *Solid State Ionics* 397, 116232 (2023).

X-rays reveal challenges in scaling up a catalyst for CO₂ hydrogenation to propane

This paper was highlighted in the industrial research section of the ESRF's annual report. It concerns a collaboration between the University of Turin (Italy), the University of Thuwal (Saudi Arabia), University of Oslo (Norway) and Haldor Topsøe (Denmark).

The valorisation of CO₂ to produce high-value chemicals such as methanol and hydrocarbons represents key technology for a future net-zero society. X-ray absorption spectroscopy was used to investigate a scaled-up PdZn/ZrO₂ + SAPO-34 catalyst for conversion of CO₂ and H₂ into propane.

The catalyst PdZn/ZrO₂ + SAPO-34 has been previously studied for the conversion of CO₂ into propane [1]. The focus of this work was to investigate if scaled-up versions of this catalyst were able to maintain the same performances as the lab-scale catalyst, considering the different preparation, which included an alumina phase as a binder to obtain tablets and extrudates.

Using X-ray absorption spectroscopy at beamline **BM31**, with the support of Fourier Transform-Infrared characterisation, the catalyst was shown to exhibit inferior performances to the lab-scale and physical mixture used as references. The physical mixture featured the presence of a PdZn alloy that was missing in both tablets and extrudates. Instead, tablets and extrudates showed the formation of Zn islands upon reduction and partial migration of Zn from the oxidic phase to the alumina binder, highlighted by the formation of Zn aluminates. The extruded catalyst showed a higher amount of Zn aluminates and showed the presence of metallic Pd, potentially leading to catalyst deactivation.

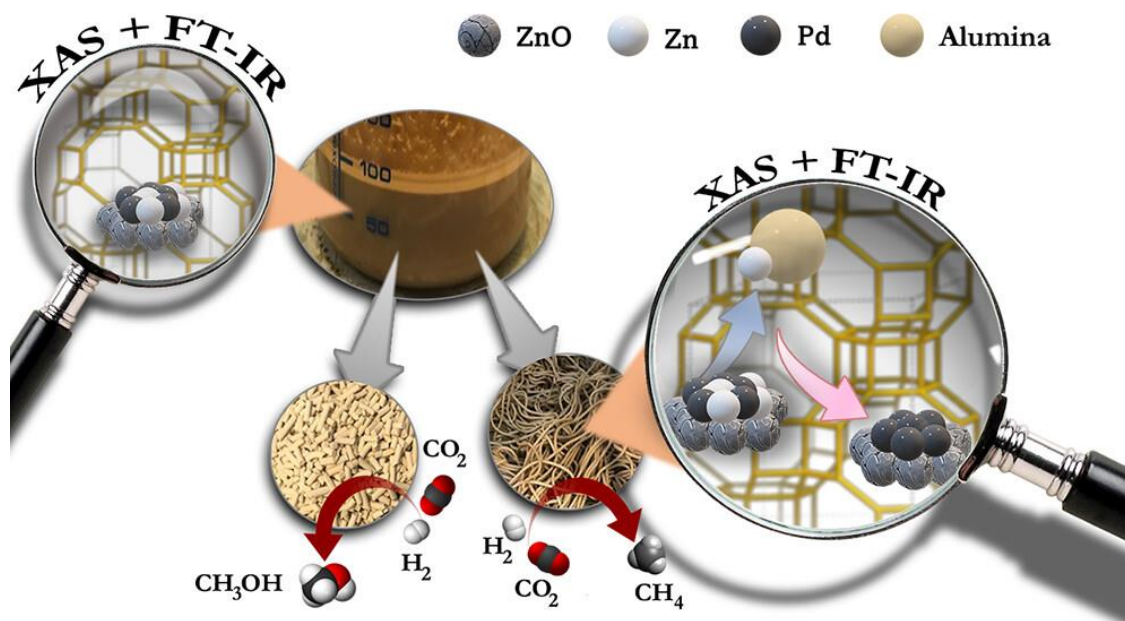


Fig. 1: X-ray absorption spectroscopy and Fourier transform-infrared characterisation was used to investigate a PdZn/ZrO₂ + SAPO-34 catalyst for conversion of CO₂ and H₂ into propane.

The findings were consistent with catalytic results, highlighting the impact of Zn aluminate formation and metallic Pd separation from the alloy on catalytic activity, with tablets showing reduced methanol conversion, due to partial deactivation of the SAPO-34, and extrudates exhibiting high methane selectivity and unconverted methanol, related to the presence of metallic Pd, maybe anchored on Zn islands. These insights

shed light on critical points that could emerge during the development of catalysts for net-zero industrial applications.

Principal publication and authors

From Lab to Technical CO₂ Hydrogenation Catalysts: Understanding PdZn Decomposition, P. Ticali (a), D. Salusso (a), A. Airi (a), S. Morandi (a), E. Borfecchia (a), A. Ramirez (b), T. Cordero-Lanzac (c), J. Gascon (b), U. Olsbye (c), F. Joensen (d), S. Bordiga (a), *ACS Appl. Mater Interfaces* 15, 5218-5228 (2023); <https://doi.org/10.1021/acsami.2c19357>

(a) Department of Chemistry, NIS Center and INSTM Reference Center, University of Turin (Italy)

(b) King Abdullah University of Science and Technology, Thuwal (Saudi Arabia)

(c) SMN Centre for Materials Science and Nanotechnology, Department of Chemistry, University of Oslo, Oslo (Norway)

(d) Haldor Topsøe, A/S Kongens Lyngby (Denmark)

Reference

[1] A. Ramirez *et al.*, *JACS Au* 1, 1719-1732 (2021).



SNBL's Outreach

Tech talk article on the ESRF frontpage



26-09-2023

New end-station for operando experiments at BM31

→ *Read more*

A new end-station at BM31 (SNBL) is now available for *in-situ* and *operando* multiprobe experiments on materials and processes for sustainable technologies and environmental applications. A novel combination of techniques enables the acquisition of complementary structural information on a material under working conditions.

The availability of experimental methods that probe a material's structure at different length and time scales is key for obtaining fundamental insights into technologically relevant materials and environmental geochemistry. Indeed, progress in sustainable technologies relies on the development of innovative materials utilising an in-depth understanding of the interplay between a material's structure and its macroscopic properties. To this end, there is a continuous need to improve X-ray-based approaches that allow the study of materials with multiple techniques during their working state (i.e., *operando* methods).

The new **BM31** beamline and end-station combines X-ray diffraction (XRD) and X-ray total scattering data for pair distribution function (PDF-TS) analysis with multi-edge X-ray absorption spectroscopy (XAS) measurements to allow the acquisition of high-quality, complementary information on a material under relevant working conditions. This covers the length-scale from short- to mid-range atomic arrangements viz. $\sim 1 \text{ \AA}$ to several nm by PDF, the average structure by XRD, as well as the electronic state and geometry around the element of interest by XAS.

The beamline's potential is illustrated by a study on the formation of single-phase, high-entropy alloy (HEA) nanoparticles as catalysts for the oxygen reduction reaction. The experiments performed at **BM31** combined *in-situ* XRD with XAS on five edges (Pt-Ir-Os-Rh-Ru), complemented with a series of *ex-situ* PDF-TS (Figure 1) and imaging experiments. This enabled a thorough investigation of the low-temperature formation of single-phase HEA nanoparticles as potential (electro-)catalysts for a series of relevant chemical reactions.

In-situ X-ray absorption near-edge structure (XANES) spectroscopy revealed the kinetics of reductions of all metals involved. It was found that Pt reduced at the lowest temperatures, followed by Os, Ir, Ru, and lastly Rh. Using XRD, the crystallisation of an fcc phase was observed at 170°C, which contracted continuously as the metals with smaller atomic radii incorporated into the alloy. At the same time, a pronounced increase in lattice strain accompanied the initial lattice contraction at lower temperatures, whereas the crystallite domains grew at higher temperatures above 350°C, where all five elements were reduced. The hcp single-phase HEA displayed a similar formation mechanism.

Rietveld analysis of the *in-situ* diffraction data indicated a pure, single-phase fcc alloy, while the refinements for the hcp-HEA could not correctly describe the ratios of Bragg peaks, indicating a very distorted and defect-rich structure for the hcp alloy. The PDF data clarified the nature of the defect-rich structure. The fast damping in the PDF-TS data (pair distances up to ca. 30 Å/fcc phase and ca. 50 Å/hcp phase) is well in line with the disordered lattices and reaffirmed the strained nature of the crystal lattice of the HEA nanoparticles.

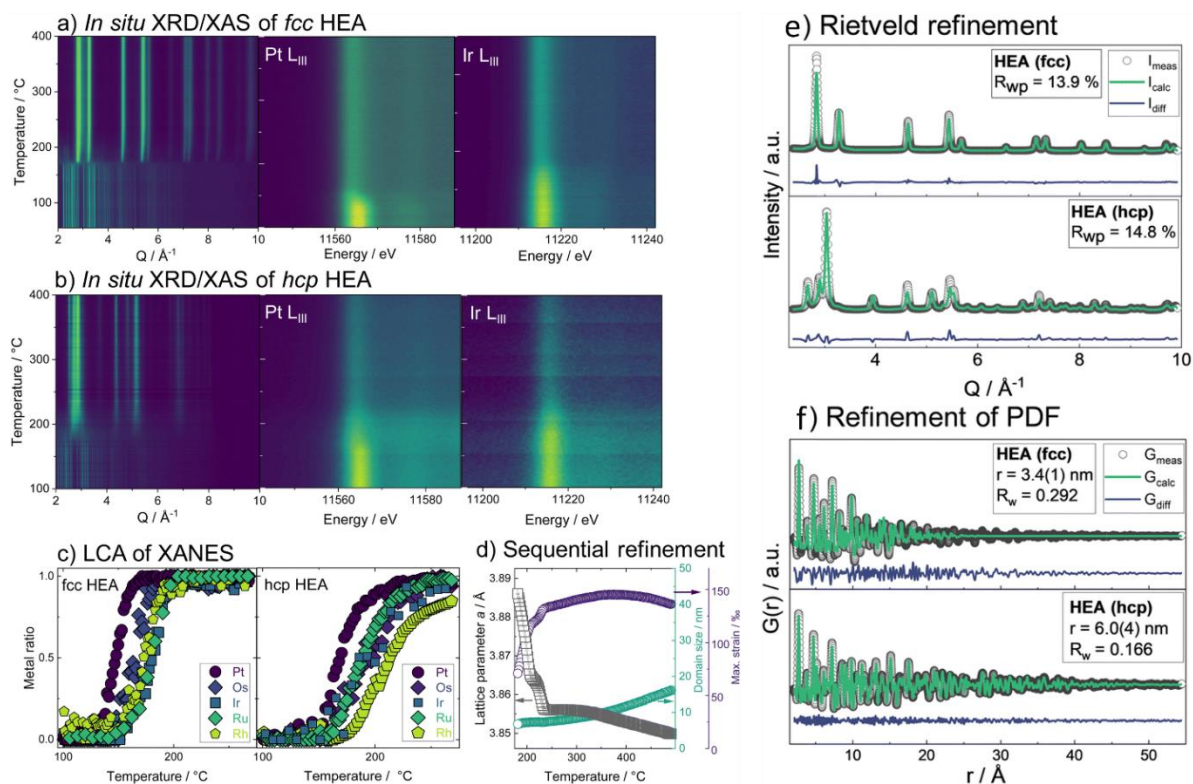


Fig 1: *In-situ* XAS-XRD studies on the formation of two different types of HEA nanoparticles (fcc and hcp) from five element mixtures. The linear combination analysis (LCA) on the XANES data and the sequential refinement (lattice parameter a , crystallite domain size and lattice strain) on the fcc HEA are displayed (a-d) and *ex-situ* Rietveld refinement of the XRD and PDF-TS refinement for the as-synthesised fcc and hcp HEA (e-f).

Overall, this study demonstrates the great potential of using the combined XAS-XRD and PDF/TS approach available at **BM31** (aided by computational simulations and advanced imaging analysis) to thoroughly explore, at the Angstrom scale, the complex and dynamic structure of industrially relevant materials under working conditions. **BM31's** capabilities can also be exploited for advanced combined studies on energy, materials, batteries and catalytic reactions.

Principal publication and authors

The more the better: on the formation of single-phase high entropy alloy nanoparticles as catalysts for the oxygen reduction reaction, R.K. Pittkowski (a), C.M. Clausen (a), Q. Chen (a), D. Stoian (b), W. van Beek (b), J. Bucher (c), R.L. Welten (c), N. Schlegel (c), J.K. Mathiesen (a,d), T.M. Nielsen (a), J. Du (c), A.W. Rosenkranz (e), E.D. Bøjesen (e), J. Rossmeisl (a), K.M.Ø. Jensen (a), M. Arenz (c), *EES. Catal.* (2023); <https://doi.org/10.1039/D3EY00201B>

(a) Center for High Entropy Alloy Catalysis (CHEAC), Department of Chemistry, University of Copenhagen (Denmark)

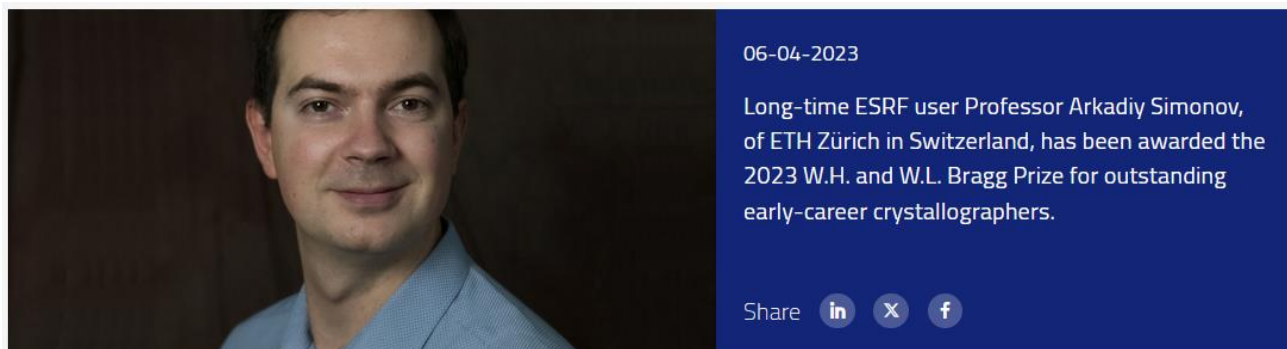
(b) Swiss Norwegian Beamlines, ESRF

(c) Department of Chemistry, Biochemistry and Pharmaceutical Sciences, University of Bern (Switzerland)

(d) Department of Physics, Technical University of Denmark (Denmark)

(e) Aarhus University, Interdisciplinary Nanoscience Center (Denmark)

ESRF and long standing SNBL user awarded 2023 Bragg prize



The prize, established by the International Union of Crystallography (IUCr) in 2017 for promising early-career researchers, recognises Professor Simonov's development of the three-dimensional difference pair distribution function (3D- Δ PDF) approach and its transformative effect on the field of materials.

A long-standing user of the CRG SNBL beamline **BM01** and ESRF beamlines ID23-1, ID22, ID15B, ID11 and ID28, Professor Simonov established the first general approach for refinement of the diffuse scattering contribution to single-crystal diffraction patterns, resulting in the development of the foremost codes for data reduction (MEERKAT) and 3D- Δ PDF refinement (YELL). He applied his methodology to a range of systems, establishing a series of proofs-of-concept and solving a number of crucially important outstanding problems in the field of complex materials.

The prize was presented during the 26th IUCr Congress in Melbourne, Australia, in August 2023, where Professor Simonov presented a Keynote Lecture on his work.



NEWS FROM THE BEAMLINES

ID19

Microtomography is available for fast access at the two tomography set-ups, both integrated in the robotic sample-changer hardware. For high resolution, pixel sizes of $0.6\ \mu\text{m}$ ($10\times/0.3\text{NA}$) and $0.3\ \mu\text{m}$ ($20\times/0.4\text{NA}$) are available (photon energies of 19 keV, 26 keV and 35 keV). For medium resolution, pixel sizes of $1.2\ \mu\text{m}$ ($5\times/0.14\text{NA}$) and $2.2\ \mu\text{m} / 3.1\ \mu\text{m}$ and $6.4\ \mu\text{m}$ ($3\times$, $2.1\times$, $1\times$ Hasselblad) are offered (again, 19 keV, 26 keV and 35 keV as well as pink wiggler configurations). Scientists mail in their samples and use a sample-changer robot and remote desktop to carry out the scans. Please contact the beamline staff for more information.

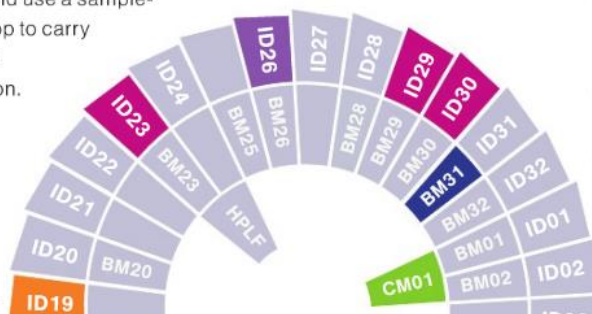
ID26

The hard X-ray emission spectrometer has been upgraded from a single-element photon-counting to a Pilatus 100 k pixel detector while maintaining on-the-



BM31

A unique new end-station (left) provides combined XRD-PDF with multi-edge XAS measurements. The optics and end-station work seamlessly together and switch automatically between configurations, allowing the acquisition of high-quality and highly complementary information under relevant working conditions in a single experiment. The detection systems include a CdTe Pilatus 2M, 16 pre-filled ion chambers and several fluorescence detectors. Dedicated ancillary equipment is available for e.g. heterogeneous catalytic and battery/electrochemistry experiments.



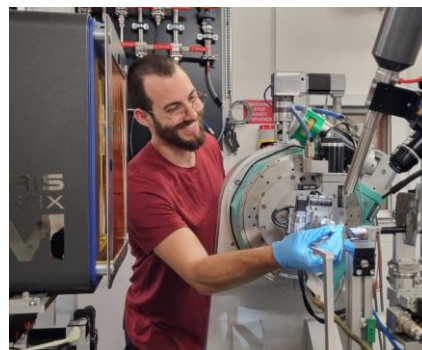
CM01

Cryo-electron tomography (cryo-ET) is an advanced imaging technique allowing the visualisation and study of

Swiss Summer School on Diffraction and Crystallography, BM01-ESRF

The first Swiss SNBL at ESRF BM01 Summer School on Diffraction and Crystallography was held in Grenoble, 05-09 June 2023. The school was proposed by Swiss members of the Swiss-Norwegian Council Wendy Lee Queen (EPFL) and Paula Abdala (ETHZ), who also organized financial support and educational certification. Sixteen students from ETHZ and EPFL attended the school to explore the theoretical and practical aspects of advanced structural characterization of crystals, powders and thin films. The school included lectures, tutorials and practical exercises demonstrating the benefits of synchrotron diffraction data for various facets of materials science. At lectures organized by BM01 staff, students got familiar with the basics of synchrotron science, diffraction and crystallography. Particular attention was paid to the information content of diffraction data, data processing, in-situ and operando experiments. The students also presented their research projects, the presentations were followed by a discussion on the possible diffraction experiments that could help answering the underlying scientific questions. As a part of practical exercises, the students measured their own samples including in-situ structural evolution of powder materials during a chemical reaction, textured films of MOFs and solar cell compounds, and single crystals with correlated disorder. The students were hence exposed to a wide variety of projects, the final lesson was allocated for a discussion on how to write and submit proposals for synchrotron experiments.

The portfolio of experimental techniques available at BM01 currently includes a set of synchrotron diffraction tools such as small-angle scattering, wide-angle scattering, high resolution diffraction, reciprocal and direct space diffraction mappings. We hope that the School helps Swiss material scientists to benefit from these synchrotron tools in their research. More information can be found at www.snbl.eu. Proposal deadlines are 1st of March and 10th of September.





Dr. Diana Piankova, postdoctoral researcher at ETH Zurich
Department of Mechanical and Process Engineering

“The synchrotron school at ESRF in Grenoble, organized by enthusiastic scientists from BM01, provided a rare opportunity to learn about synchrotron techniques through informative lectures and hands-on experience in sample measurements. Not only were we able to perform high-resolution powder diffraction, GIXRD, and single crystal measurements on our samples, but we also had the chance to conduct in situ experiments under a gas environment with the necessary high temporal resolution to probe the kinetics of different processes.

As an electron microscopist, I found this school particularly valuable. It allowed me to expand my expertise beyond electron radiation-based methods and provided insights into implementing synchrotron techniques in my research, enabling a multiscale understanding of functional materials. By the end of the school, we had gained knowledge of the capabilities of the BM01 beamline for studying our materials, laying a strong foundation for future proposal planning and identifying the research questions that can be effectively addressed using synchrotron radiation. We are extremely grateful for this experience, made possible by the exceptional team of Dmitry, Chloe, and Charlie, who shared their knowledge and provided their support and help throughout the school.”

PhD student Ghewa Alsabeh
EPFL Laboratory of Photonics and Interfaces and Smart Energy Materials, Adolphe Merkle Institute, University of Fribourg

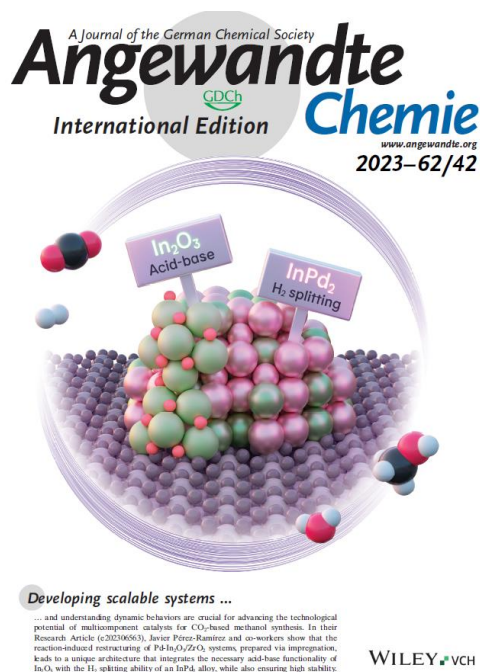
“The synchrotron summer school was a one of a kind experience for me! It was the first time I ever saw and worked with such a big and powerful synchrotron. Seeing how these measurements take place in real life was amazing and prepared me well for my next beamtime application and measurements!

Such a high-brilliance photon beam allowed me to learn more information about the perovskites I am studying due to the high accuracy of light diffraction from it. I was able to prove the formation of 2D phase, study the phase purity, the orientation of the materials and get much more information.

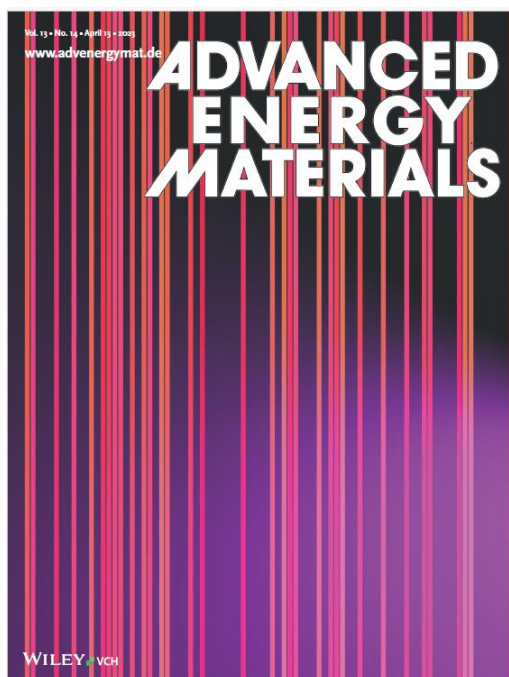
Besides this, I had the chance to engage with a team of experts in the field to discuss my project and the obstacles I am facing for a better understanding of my material. Huge thanks go to BM01 staff for their assistance not only during the school but also in the after-school follow-ups!”

SNBL publications on journal covers

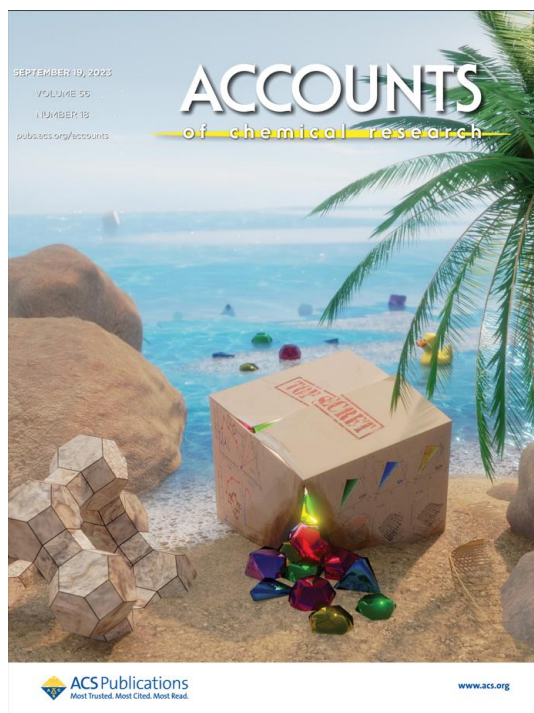
Araujo, T.P., Morales-Vidal, J., Giannakakis, G., Mondelli, C., Eliasson, H., Errni, R., Stewart, J.A., Mitchell, S., Lopez, N., Perez-Ramirez, J. *Reaction-Induced Metal-Metal Oxide Interactions in Pd-In₂O₃/ZrO₂ Catalysts Drive Selective and Stable CO₂ Hydrogenation to Methanol* [Ang. Chemie, e202306563, 2023](https://doi.org/10.1002/ange.202306563)



Araujo, T.P., Morales-Vidal, J., Zou, T., Agrachev, M., Verstraeten, S., Willi, P.O., Grass, R.N., Jeschke, G., Mitchell, S., Perez-Ramirez, J. *Design of Flame-Made ZnZrO_x Catalysts for Sustainable Methanol Synthesis from CO₂* [Adv. Energy Materials, 13, 4, 2204122, 2023](https://doi.org/10.1002/aem.2204122)



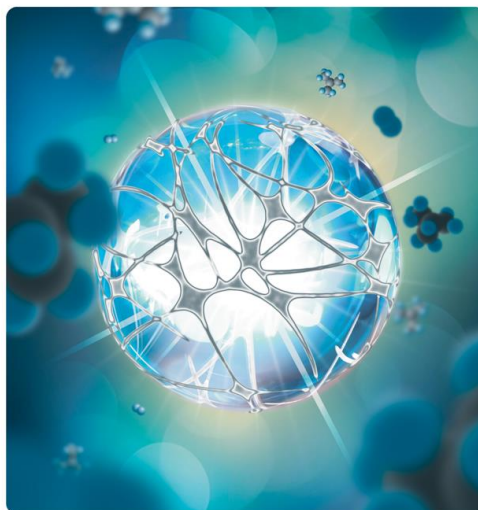
Asselman, K., Kirschhock, C., Breynaert, E. *Illuminating the Black Box: A Perspective on Zeolite Crystallization in Inorganic Media* [Acc. Chem. res.](#), **56**, 18, 2391-2402, 2023



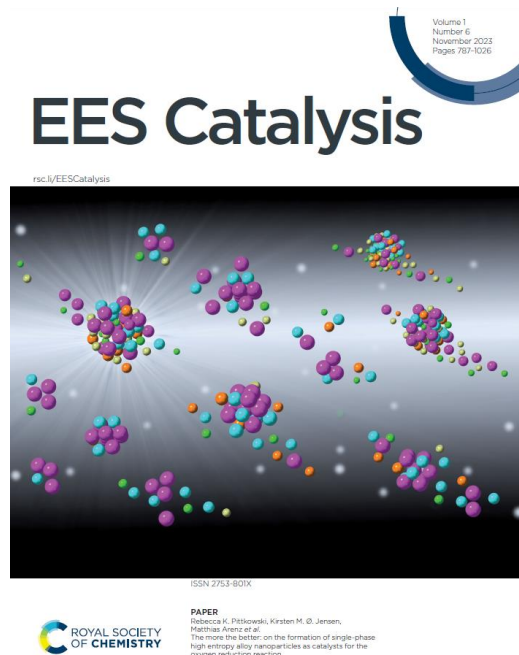
Chen, Z., Zimmerli, N.K., Zubair, M., Yakimov, A.V., Björgvinsdóttir, S., Alaniva, N., Willinger, E., Barnes, A.B., Bedford, N.M., Copéret, C., Florian, P., Abdala, P.M., Fedorov, A., Müller, C.R. *Nature of GaO_x Shells Grown on Silica by Atomic Layer Deposition* [Chem. Mater.](#), **35**, 18, 7475-7490, 2023

cm CHEMISTRY OF MATERIALS

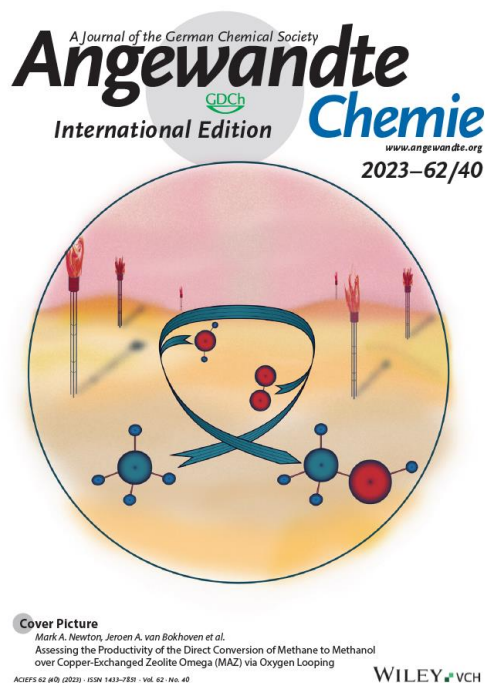
SEPTEMBER 26, 2023 | VOLUME 35 | NUMBER 18 | pubs.acs.org/cm



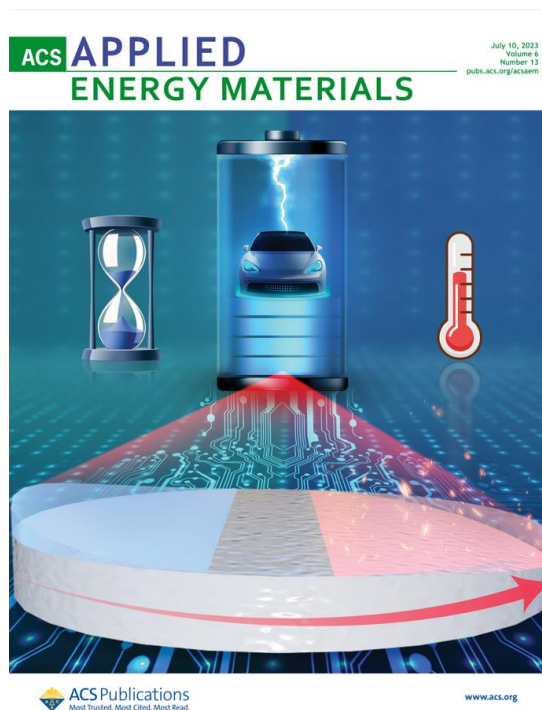
Pittkowski, R.K., Clausen, C.M., Chen, Q., Stoian, D.C., van Beek, W., Bucher, J., Welten, R.L., Schlegel, N., Mathiesen, J.K., Nielsen, T.M., Du, J., Rosenkranz, A.W., Bojesen, E.D., Rossmeisl, J., Jensen, K.M.O., Arenz, M. *The more the better: on the formation of single-phase high entropy alloy nanoparticles as catalysts for the oxygen reduction reaction* [EES. Catal., 1, 950-960, 2023](#)



Wieser, J., Knorpp, A.J., Stoian, D.C., Rzepka, P., Newton, M.A., van Bokhoven, J.A. *Assessing the Productivity of the Direct Conversion of Methane-to-Methanol over Copper-Exchanged Zeolite Omega (MAZ) via Oxygen Looping* [Ang. Chemie, e202305140, 2023](#)



Zhang, H., Paggiaro, G., Okur, F., Huwiler, J., Cancellieri, C., Jeurgens, L.P.H., Chernyshov, D., van Beek, W., Kovalenko, M.V., Kravchyk, K.V. *On High-Temperature Thermal Cleaning of $\text{Li}_7\text{La}_3\text{Zr}_2\text{O}_{12}$ Solid-State Electrolytes* [ACS Appl. Energy Mater.](#), 6, 13, 6972-6980, 2023



Involvement of SNBL in ESRF STREAMLINE cross-cut review

A cross-cut review is part of the ESRF's STREAMLINE Work Package 2 aiming to produce a sustainable business plan through a wide-ranging review of scientific opportunities with strong socio-economic impact. STREAMLINE is a Horizon2020 funded project that complements the ESRF-EBS upgrade by enhancing user operation through new procedures and systems. STREAMLINE is a grant worth 5 million Euros for which the ESRF is the sole beneficiary. STREAMLINE runs for four years from 15 November 2019. The external research groups present at the ESRF, like the SNBL, are also part of such reviews. The findings of the reviews will inform the steering and prioritisation of the future ESRF medium- and long-term scientific programme, particularly in exploiting the ESRF-EBS opportunities. This advice will be used to inform prioritisation of new beamlines, of technology developments, of instrument upgrades and refurbishments, of user service developments, as well as to develop enhanced outreach programmes towards fledgling or new user communities. The topic of review in question was: *Catalysis and industry: past and future activities at the ESRF*, one of SNBL's strengths. From the review it turned out that BM31 has the highest output from all ESRF beamline in this field, BM01 is ranked 4th. Both SNBL beamlines together have produced 20% of all catalyst related research at the ESRF. The figure below shows the analysis of all relevant papers per beamline.

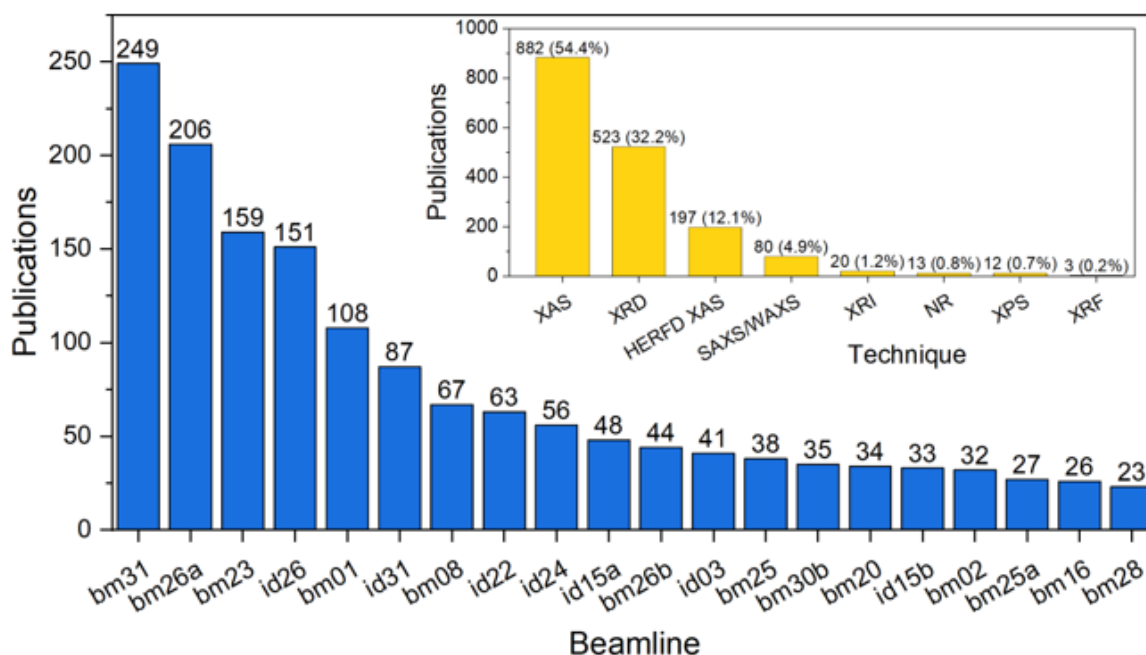


Figure 3.5 Breakdown of the ESRF publications in the field of catalysis published in 2011-2022 by experimental stations (top 20 beamlines) and techniques. In case a beamline changed the beam port in the covered period, the old and new numbers of publications are summed and showed under the current beamline name, as it is the case for BM31 (previously BM01b), BM01 (previously BM01a) and BM23 (previously BM29).

Development of enabling technologies

SNBL is continuously developing its instrumentation to provide unique, new and efficient experimental opportunities answering to the needs of our user community. SNBL has recognized at a very early stage (over 15 years ago) the importance of software for data treatment and analysis as an integrated service to the community. SNBL has continued its very successful software development program in 2023 and the software is used on at least 3 synchrotrons and 8 beamlines. On the hardware side; new detector mechanics for BM01 were designed to enable SAXS-WAXS experiments. As instruments get faster and evolve the sample environment have to follow suit. Special emphasis was therefore put on the development of professional sample environments to optimally exploit the new instruments.

BM01 SAXS/WAXS design and procurement

On BM01 the major job was designing a new support for the WAXS detector and a flight tube for the direct beam path going to the SAXS detector. The are no gaps in the diffraction signal as the highest angle on the SAXS detector is above the smallest angle on the WAXS detector. All parts have been ordered in 2023.

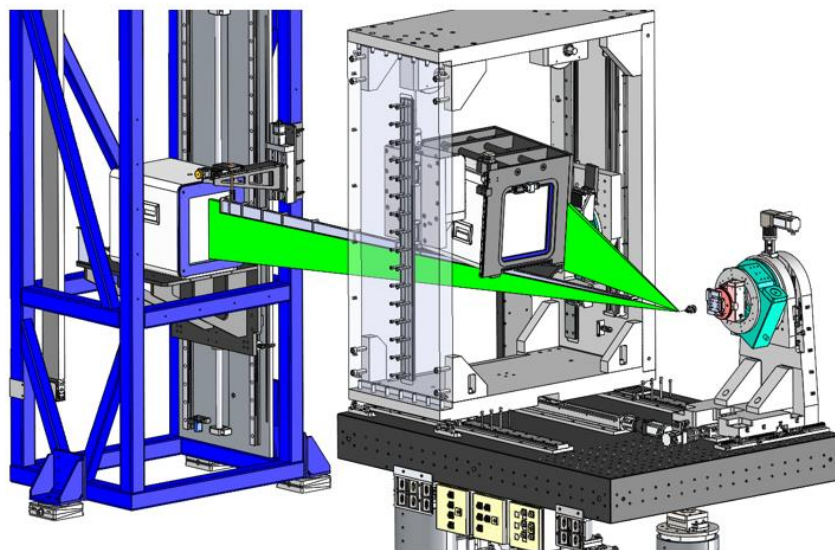


Figure 1. Two detectors installed with the new wide-angle detector mount and SAXS flight tube.

Software developments

SNBL provides, for many years now, open source software to its users and to a broader scientific community. It can be downloaded on the following page <https://soft.snbl.eu/>

There are various software suits available for:

1. beamline control
2. various types of data conversion
3. fast on-line powder integration
4. visualisation and frequency analysis for modulation-enhanced powder diffraction
5. refinement of absolute structure
6. Inspection and geometric Ewald sphere corrections of GISAXS and GIWAXS data
7. Sequential refinement of multiple single crystal datasets with Crysalis and shelx
8. New in 2023: pole figure reconstruction from 2D data

In 2023 an analysis tool for the calculation of texture maps from powder diffraction data for polycrystalline materials and thin films has been developed. The algorithm performs 3 steps. First BUBBLE does the integration over user-specified 2Theta range and calculates patterns of azimuthal intensity distribution. Second, all the azimuthal patterns collected at different orientations of the sample are read with MEDVED to make 2D maps of intensity distribution in 2Theta. Third, the 2D map is transformed into a pole figure with a separate Python script.

The software is described in the following paper: J. Synchrotron Rad. (2016). 23, 825-829 and has received 70 citations in 2023 for a total of 370. It appears from the 370 citations that SNBL software is installed and used at at least 8 beamlines spread over three synchrotrons. BM01, BM31, BM14, BM26, BM20 and ID28 at the ESRF. Materials Science beamline at Swiss light source and NCD-SWEET at ALBA.

Sample environment development program

After the major infrastructural changes on BM31, developed and implemented in 2021 and 2022, 2023 has very much been focussed on enhancing the sample environmental capabilities for both BM01 and BM31. The sample environment is crucial in today's synchrotron science programs as almost all experiments are performed as a function of some external stimuli, temperature and/or pressure and/or gas environment. To cater for the continuously evolving science performed by our users, SNBL has set out a massive development program in this area. Seven different sample environments have been further optimized or newly designed and rolled out to the user program. Three high impact publications from 2023 can already be associated with the new developments (Gelpi *et.al.* 2023, Zhang *et.al.* 2023, Zhang *et.al.* 2023) respectively in Advanced Materials IF 29.4, Applied Energy Materials IF 27.8 and Advanced Science IF 15.1, thus underlining the importance of this development program.

XAFS-XRD Catalysis high temperature and pressure micro flow reactor

On BM31 a major part of the research program is in the field of heterogeneous catalysis. The capabilities, reliability and operational efficiency are continuously being challenged by our users. A second design iteration was therefore made on the first version of the reaction cell now also implementing fast switching valves, reduced dead volume, increase the capabilities for large diameter samples and ensure the chemical integrity of the system. The improved design can be seen in figure 1,

All parts are currently being manufactured. More than 50% of BM31 experiments are being performed with this system and the majority of BM31 publication are done with this device.

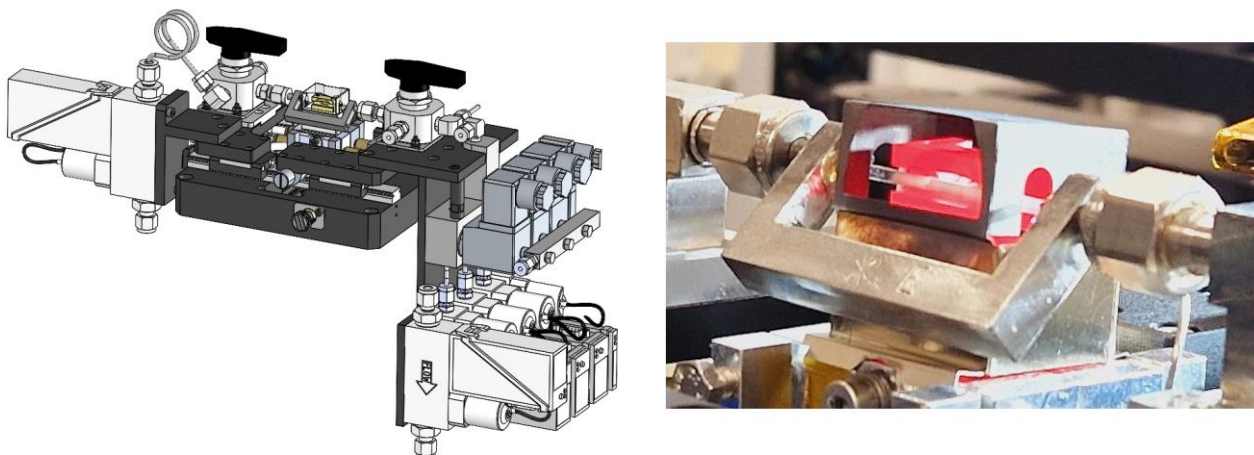


Figure 1. Improved Catalysis high temperature and pressure micro flow reactor (Picture courtesy of Magnus Rønning)

1st XRD Ultra-fast high temperature heater 1100°C

A general method to synthesize and sinter bulk ceramics in seconds has recently appeared in literature. Synthesizing ceramics can require heating for long times at high temperatures, this makes high-through-put screening of new materials challenging. Wang *et al.* developed a new ceramic-sintering technique by ramping up and ramp down the temperature quickly. Ultrafast sintering is much better suited for synthesizing many compositions and screen for optimized properties for a variety of applications, including the development of new solid-state electrolytes. (Wang *et al.* 2020). SNBL's developed heater (Marshall *et al.* 2023), see figure 2, has been used successfully by our users for various studies on sintering solid state battery materials (Zhang *et al.* 2023, Zhang *et al.* 2023).

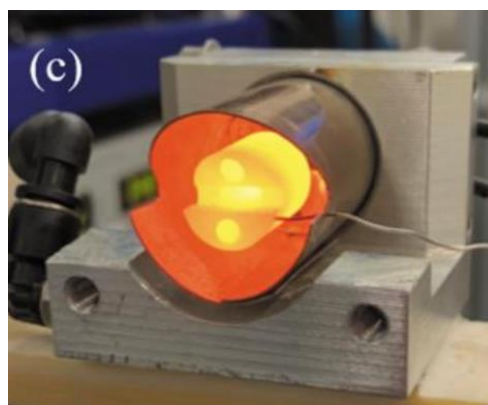


Figure 2. SNBL's new high temperature, high heating rate, low axial gradient capillary heater

2nd XRD Ultra-fast high temperature heater 1300°C (NTNU – ELKEM – SNBL)

Thanks to the success of the new heater a 2nd development cycle has been initiated to push the performance limits. This development was especially targeted for, and partially financed by an NTNU user group working in close contact with ELKEM, a Norwegian supplier for silicon and carbon-based materials and foundry alloys. With respect to the first furnace, notably the maximum temperature and ramp speed have been improved now reaching 1300°C and 100°C/min. See figure 3. The increased performance came at the expense of the size of the hot zone. Both furnaces complement each other and are readily available for our users.

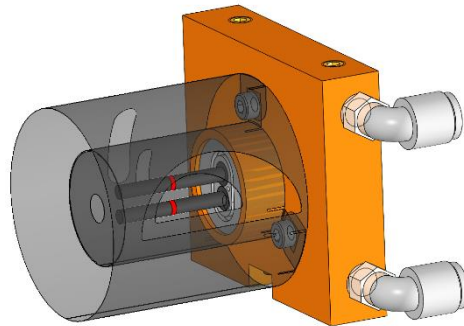


Figure 3. SNBL's 2nd high temperature furnace with increased maximum temperature and ramp rates.

Total Scattering operando liquid electrolyte battery cell (Uni Oslo – SNBL)

Silicon has been recognized as a promising anode material for next generation Li-ion batteries. It's therefore crucial to understand the lithiation and delithiation reaction pathways. The task is demanding due to the amorphous nature of Si and the complexity of the phases formed during the charge and discharge processes. Due to the amorphous nature pair distribution function (PDF) analysis of X-ray total scattering, recently added to BM31, is the analysis method of choice. A dedicated operando cell to this extend (see figure 4) was developed with users from the University of Oslo and successfully tested on the ESRF's ID11 beamline (see figure 5).

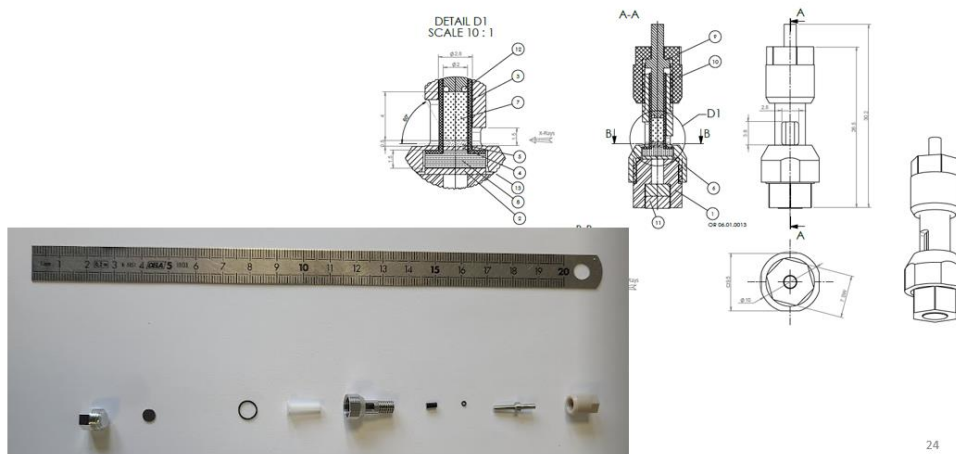


Figure 4. Design of SNBL's and UiO's total scattering operando battery cell

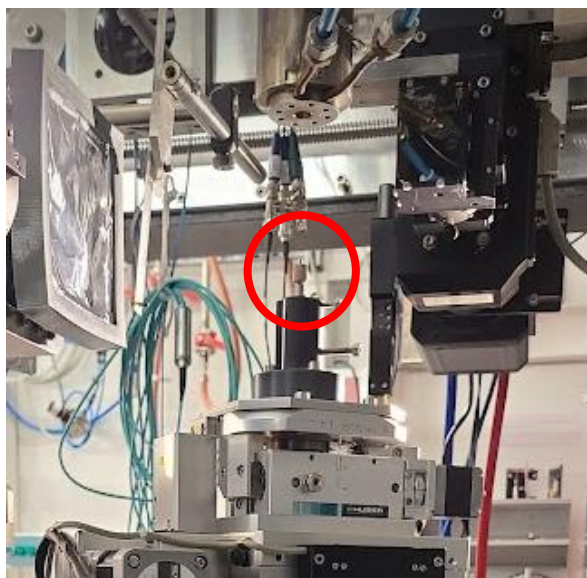


Figure 5. SNBL's and UiO's total scattering operando battery cell in action on ID11

XAFS-XRD operando Solid State Battery cell (NTNU – SNBL)

Solid-state batteries are most promising among energy storage systems for achieving high energy density and safety. There are challenges/issues that need further research to enhance the SSBs performance before adopting them to large-scale applications. These include, amongst others, mechanical and chemical stability, ionic transport, interfacial resistance, stress, cracking and Li dendrite growth. A Solid-State Battery cell has been developed (See figure 6) and successfully tested together with a group from the NTNU (See figure 7). It is foreseen that the cell will be employed to study chemical, structural, and microstructural changes under different stack pressure, temperature and charge-discharge rate by using operando XRD/XANES. It's particularly satisfying that the SSB cell has been the catalyser for a Norwegian-Swiss collaboration between researchers from the NTNU and ETHZ/EMPA.

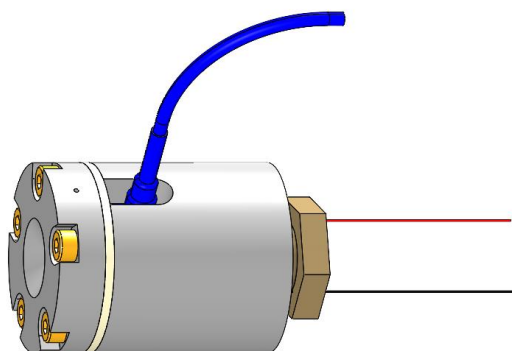


Figure 6. Design of SNBL's and NTNU XAFS-XRD operando Solid State Battery cell

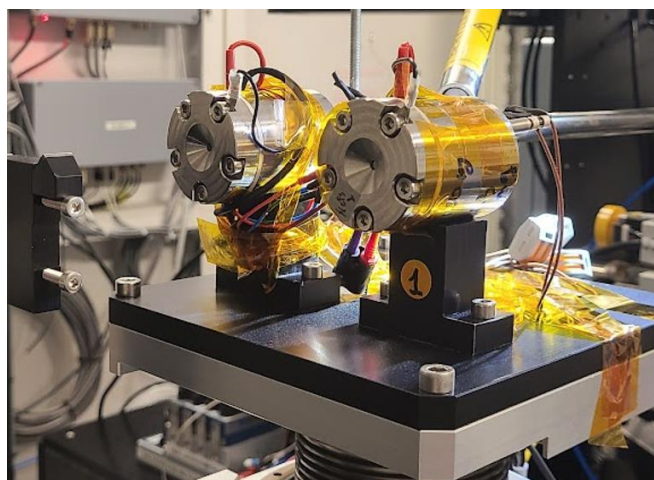


Figure 7. First experiment with SNBL's and NTNU XAFS-XRD operando Solid State Battery cell on BM31

EXAFS/XRD/PDF operando electrochemistry cell (Uni Bern – SNBL)

High entropy alloys (HEAs) are an important new material class with significant application potential in catalysis and electrocatalysis. For instance, the efficiency of green hydrogen production very much depends on the scientific breakthroughs in electrocatalysis. The new capabilities of BM31 have already been exploited to study the synthesis of HEA materials with unprecedented detail (Pittkowski *et.al.* 2023), see also the tech talk article earlier in this annual report. SNBL has now also developed, with the researchers from Bern university, an electrochemistry cell that will be capable of studying the newly synthesized materials in their working environment. The cell is capable of making optimum use of BM31 unique capabilities combining low energy EXAFS with high energy Total Scattering data acquisitions. The new cell (see Figure 8) therefore features a low energy EXAFS detector uniquely integrated in the electrochemistry cell. The cell is currently in production and experiments are planned.

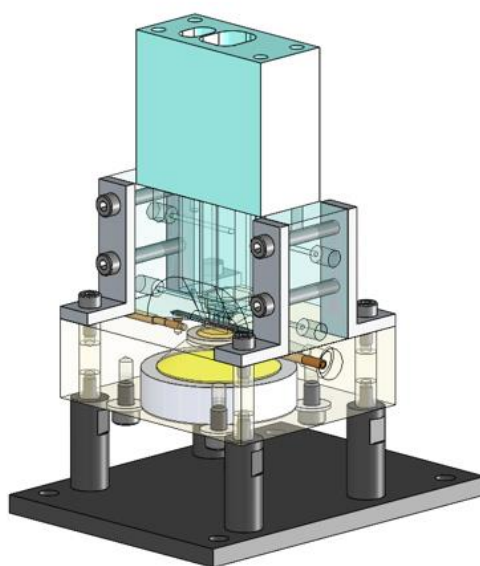


Figure 8. SNBL's and UniBern EXAFS/XRD/PDF operando electrochemistry cell

XRD 1000 Bar Sapphire Capillary Cell

Phase change materials for energy transport and solid-state refrigeration are currently operating/investigated in a pressure window that ranges from 0 to 2kbar. In the current synchrotron high pressure landscape there is a gap in the available pressure range. Sub ~ 150 bar experiments can be readily performed with capillary gas pressure cells. Diamond Anvil cell starts to hit their stride above 2 to 3 kbar. The new XRD 1000 Bar Sapphire Capillary Cell (SCC) fills in the gap and allows collecting isobars and isotherms from 0-1000 bar and 220 to 500K (see Figure 9). The SCC is fully implemented in the control software allowing e.g. automated isotherms (see Figure 10). The SCC is complementary to high pressure differential scanning calorimetry operating in a similar pressure and temperature window. The cell has also attracted interest from the porous material community investigating MOFs and water inclusion of clays. The applications of SCC are broad and obviously still developing. The industrially highly relevant temperature and pressure window was previously inaccessible with diffraction and finds applications in chemistry and materials science. Two publications have already appeared in 2023 (Gelpi *et.al.* 2023, Muscarella *et.al.* 2023) with the new device.

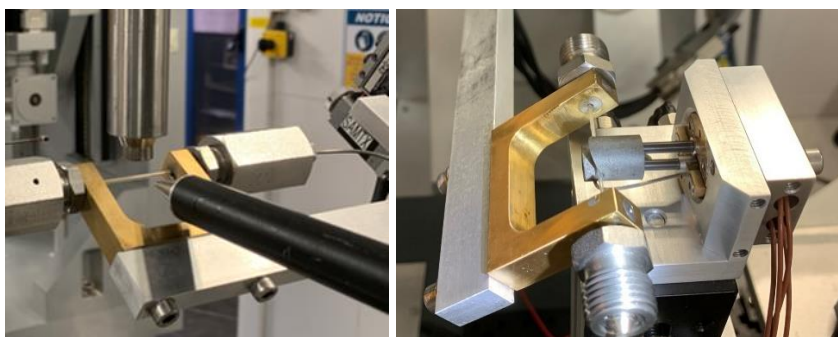


Figure 9. XRD 1000 Bar Sapphire Capillary Cell installed on BM01

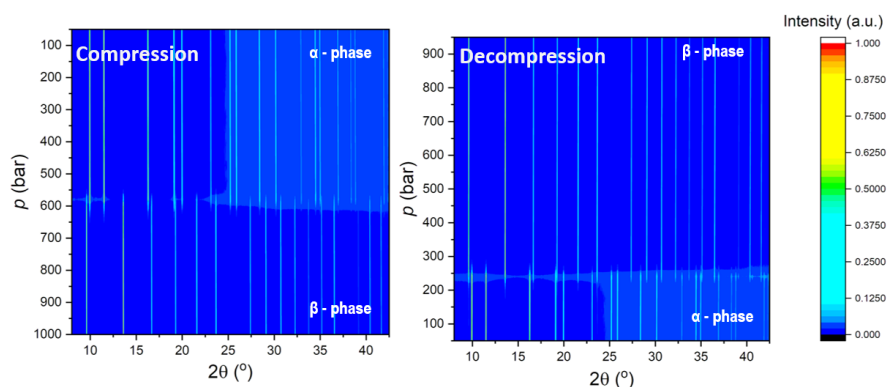


Figure 10. XRD in pressure cell; automated isotherms (@290K) with a pattern approximately every 10 bar

References related to sample environment developments

Chengwei Wang et al. *A general method to synthesize and sinter bulk ceramics in seconds*. Science 368,521-526(2020). DOI:10.1126/science.aaz7681

Gelpi, M., García-Ben, J., Rodríguez-Hermida, S., López-Beceiro, J., Artiaga, R., Baaliña, A., Romero-Gómez, M., Romero-Gómez, J., Zaragoza, S., Salgado-Beceiro, J., Walker, J., McMonagle, C.J., Castro-García, S., Sánchez-Andújar, M., Señarís-Rodríguez, M.A., Bermúdez-García, J.M. *Empowering CO₂ Eco-Refrigeration With Colossal Breathing-Caloric-Like Effects in MOF-508b* Adv. Mater., 2310499, 2023

Marshall, K.P., Emerich, H., McMonagle, C.J., Fuller, C.A., Dyadkin, V., Chernyshov, D., van Beek, W. *A new high temperature, high heating rate, low axial gradient capillary heater* J. of Synchrotron Radiation, 30, 267-272, 2023

L. A. Muscarella, H. J. Jöbss, B. Baumgartner, P. T. Prins, D. N. Maaskant, A. V. Petukhov, D. Chernyshov, C. J. McMonagle, E. M. Hutter, *Which Ion Dominates the Temperature and Pressure Response of Halide Perovskites and Elpasolites?*, The Journal of Physical Chemistry Letters 2023, 14, 9042-9051.
<https://pubs.acs.org/doi/full/10.1021/acs.jpcllett.3c02403>

Pittkowski, R.K., Clausen, C.M., Chen, Q., Stoian, D.C., van Beek, W., Bucher, J., Welten, R.L., Schlegel, N., Mathiesen, J.K., Nielsen, T.M., Du, J., Rosenkranz, A.W., Bojesen, E.D., Rossmesl, J., Jensen, K.M.O., Arenz, M. *The more the better: on the formation of single-phase high entropy alloy nanoparticles as catalysts for the oxygen reduction reaction* EES. Catal., 1, 950-960, 2023

Zhang, H., Okur, F., Cancellieri, C., Jeurgens, L.P.H., Parrilli, A., Karabay, D.T., Nesvadba, M., Hwang, S., Neels, A., Kovalenko, M.V., Kravchyk, K.V. *Bilayer Dense-Porous Li₇La₃Zr₂O₁₂ Membranes for High-Performance Li-Garnet Solid-State Batteries* Adv. Sci., 2205821, 2023

Zhang, H., Paggiaro, G., Okur, F., Huwiler, J., Cancellieri, C., Jeurgens, L.P.H., Chernyshov, D., van Beek, W., Kovalenko, M.V., Kravchyk, K.V. *On High-Temperature Thermal Cleaning of Li₇La₃Zr₂O₁₂ Solid-State Electrolytes* ACS Appl. Energy Mater., 6, 13, 6972-6980, 2023

Scientific output Impact Factors

67 peer reviewed papers were published in 2023 containing data from SNBL. 30% of the SNBL publications are published in journals with an impact factor above 10 and 80% above impact factor 4. See below the detailed distribution of papers per journal in 2023 and their impact factor.

Journal	Journal Impact Factor	Web of Science Documents
NATURE MATERIALS	41.2	1
ADVANCED MATERIALS	29.4	2
ADVANCED ENERGY MATERIALS	27.8	2
ACCOUNTS OF CHEMICAL RESEARCH	18.3	1
ANGEWANDTE CHEMIE-INTERNATIONAL EDITION	16.6	5
NATURE COMMUNICATIONS	16.6	1
ADVANCED SCIENCE	15.1	2
CHEMICAL ENGINEERING JOURNAL	15.1	1
JOURNAL OF THE AMERICAN CHEMICAL SOCIETY	15	3
ACS CATALYSIS	12.9	1
JOURNAL OF MATERIALS CHEMISTRY A	11.9	1
JOURNAL OF MATERIALS SCIENCE & TECHNOLOGY	10.9	1
ACS APPLIED MATERIALS & INTERFACES	9.5	4
ACTA MATERIALIA	9.4	1
CELL REPORTS PHYSICAL SCIENCE	8.9	2
CHEMISTRY OF MATERIALS	8.6	3
CHEMICAL SCIENCE	8.4	3
APPLIED MATERIALS TODAY	8.3	1
JOURNAL OF CATALYSIS	7.3	1
ACS PHOTONICS	7	1
NANOSCALE	6.7	1
ACS APPLIED ENERGY MATERIALS	6.4	1
JOURNAL OF PHYSICAL CHEMISTRY LETTERS	5.7	1
ENERGY & FUELS	5.3	1
CATALYSIS TODAY	5.3	1
CATALYSIS SCIENCE & TECHNOLOGY	5	1
CHEMICAL COMMUNICATIONS	4.9	1
INORGANIC CHEMISTRY	4.6	3
MOLECULES	4.6	1
SCIENTIFIC REPORTS	4.6	1
INTERMETALLICS	4.4	1

Journal	Journal Impact Factor	Web of Science Documents
JOURNAL OF PHOTOCHEMISTRY AND PHOTOBIOLOGY A	4.3	1
DALTON TRANSACTIONS	4	1
LANGMUIR	3.9	1
TOPICS IN CATALYSIS	3.6	1
ADVANCED ENGINEERING MATERIALS	3.6	1
PHYSICAL REVIEW MATERIALS	3.4	1
EUROPEAN PHYSICAL JOURNAL PLUS	3.4	1
INORGANICS	2.9	1
INORGANICA CHIMICA ACTA	2.8	1
CRYSTALS	2.7	1
JOURNAL OF SYNCHROTRON RADIATION	2.5	1
JOURNAL OF SOL-GEL SCIENCE AND TECHNOLOGY	2.5	1
ACTA CRYSTALLOGRAPHICA SECTION B-STRUCTURAL	1.9	2
ZEITSCHRIFT FUR ANORGANISCHE UND ALLGEMEINE CHEM	1.4	1

Scientific output Research Areas

All the SNBL papers in 2023 were also categorized by research area. As the earlier years it's clear SNBL has a strong portfolio in energy related research, chemistry and materials science followed by physics and crystallography. See below the full distribution per Research Area.

Research Area	Number of publications
MATERIALS SCIENCE, MULTIDISCIPLINARY	30
CHEMISTRY, MULTIDISCIPLINARY	24
CHEMISTRY, PHYSICAL	19
NANOSCIENCE & NANOTECHNOLOGY	11
PHYSICS, APPLIED	8
CHEMISTRY, INORGANIC & NUCLEAR	7
ENERGY & FUELS	7
PHYSICS, CONDENSED MATTER	6
ENGINEERING, CHEMICAL	4
CRYSTALLOGRAPHY	3
METALLURGY & METALLURGICAL ENGINEERING	3
PHYSICS, MULTIDISCIPLINARY	3
CHEMISTRY, APPLIED	2
OPTICS	2
BIOCHEMISTRY & MOLECULAR BIOLOGY	1
ENGINEERING, ENVIRONMENTAL	1
INSTRUMENTS & INSTRUMENTATION	1
MATERIALS SCIENCE, CERAMICS	1
PHYSICS, ATOMIC, MOLECULAR & CHEMICAL	1

Involvement of industry in SNBL's publication output

One of the criteria to measure the industrial relevance of research done at SNBL is to evaluate the number of companies involved in SNBL publications. It turns out that eleven different companies are involved in a total of twelve papers. Roughly one out of five SNBL publications has an industrial partner.

1. Gelpi, M., García-Ben, J., Rodríguez-Hermida, S., López-Beceiro, J., Artiaga, R., Baaliña, A., Romero-Gómez, M., Romero-Gómez, J., Zaragoza, S., Salgado-Beceiro, J., Walker, J., McMonagle, C.J., Castro-García, S., Sánchez-Andújar, M., Señarís-Rodríguez, M.A., Bermúdez-García, J.M. *Empowering CO₂ Eco-Refrigeration with Colossal Breathing-Caloric-Like Effects in MOF-508b* Adv. Mater., 2310499, 2023



2. Redekop, E.A., Cordero-Lanzac, T., Salusso, D., Pokle, A., Oien-Odegaard, S., Sunding, M.F., Diplas, S., Negri, C., Borfecchia, E., Bordiga, S., Olsbye, U. *Zn Redistribution and Volatility in ZnZrO_x Catalysts for CO₂ Hydrogenation* Chem. Mater., 35, 24, 10434-10445, 2023



3. Gopakumar, J., Benum, P.M., Svenum, I.-H., Enger, B.C., Waller, D., Ronning, M. *Redox transformations of Ru catalyst during NO oxidation at industrial nitric acid production conditions* Chem. Engineering J., 475, 146406, 2023



4. Gopakumar, J., Vold, S., Enger, B.C., Waller, D., Vullum, P.E., Ronning, M. *Catalytic oxidation of NO to NO₂ for industrial nitric acid production using Ag-promoted MnO₂/ZrO₂ catalysts* Catal. Sci. Technol., 13, 2783-2793, 2023



5. Kvande, K., Garetto, B., Deplano, G., Signorile, M., Solemsli, B.G., Prodinge, S., Olsbye, U., Beato, P., Bordiga, S., Svelle, S., Borfecchia, E. *Understanding C–H activation in light alkanes over Cu-MOR zeolites by coupling advanced spectroscopy and temperature-programmed reduction experiments* Chem. Sci., 14, 9704-9723, 2023



6. Ticali, P., Salusso, D., Airi, A., Morandi, S., Borfecchia, E., Ramirez, A., Cordero-Lanzac, T., Gascon, J., Olsbye, U., Joensen, F., Bordiga, S. *From lab to technical CO₂ hydrogenation catalysts: understanding PdZn decomposition* ACS Appl. Mater. Interfaces, 15, 4, 5218-5228, 2023



7. X. Zhou, G. A. Price, G. J. Sunley, C. Copéret, *Small Cobalt Nanoparticles Favor Reverse Water-Gas Shift Reaction Over Methanation Under CO₂ Hydrogenation Conditions* Ang. Chem. Int. Ed. 2023, 62, e202314274.



8. Araujo, T.P., Morales-Vidal, J., Giannakakis, G., Mondelli, C., Eliasson, H., Erni, R., Stewart, J.A., Mitchell, S., Lopez, N., Perez-Ramirez, J. *Reaction-Induced Metal-Metal Oxide Interactions in Pd-In₂O₃/ZrO₂ Catalysts Drive Selective and Stable CO₂ Hydrogenation to Methanol* Ang. Chemie, e202306563, 2023



9. Sexton, A., Kanters, M., Demchenko, H., Pacáková, B., Fossum, J.O., Balzano, L. and Knaapila, M. *Classifying Tensile Loading History of Continuous Carbon Fiber Composites Using X-Ray Scattering and Machine Learning* Adv. Eng. Mater., 26, 2301415, 2023



10. Lätsch, L., Kaul, C.J., Yakimov, A.V., Müller, I.B., Hassan, A., Perrone, B., Aghazada, S., Berkson, Z.J., de Baerdemaeker, T., Parvulescu, A.-N., Seidel, K., Teles, J.H., Copéret, C. *NMR Signatures and Electronic Structure of Ti Sites in Titanosilicalite-1 from Solid-State $^{47/49}\text{Ti}$ NMR Spectroscopy* J. Am. Chem. Soc., 145, 28, 15018-15023, 2023



11. Zhang, W., Ma, H., Wang, Y., Regli, S.K., Ronning, M., Rout, K.R., Margossian, T., Chen, D. *In situ monitoring of dynamic behavior of La-doped $\text{CuCl}_2/\gamma\text{-Al}_2\text{O}_3$ catalyst in ethylene oxychlorination* J. of Catalysis, 417, 314-322, 2023



12. Loughran, R.P., Hurley, T., Gladysiak, A., Chidambaram, A., Khivantsev, K., Walter, E.D., Graham, T.R., Reardon, P., Szanyi, J., Fast, D.B., Miller, Q.R.S., Park, A.-H.A., Stylianou, K.C. *CO_2 capture from wet flue gas using a water-stable and cost-effective metal-organic framework* Cell Reports Physical Science, 4, 7, 101470, 2023



Publication list 2023

1. Araujo, T.P., Morales-Vidal, J., Giannakakis, G., Mondelli, C., Eliasson, H., Erni, R., Stewart, J.A., Mitchell, S., Lopez, N., Perez-Ramirez, J. *Reaction-Induced Metal-Metal Oxide Interactions in Pd-In₂O₃/ZrO₂ Catalysts Drive Selective and Stable CO₂ Hydrogenation to Methanol* [Ang. Chemie, e202306563, 2023](#)
2. Araujo, T.P., Morales-Vidal, J., Zou, T., Agrachev, M., Verstraeten, S., Willi, P.O., Grass, R.N., Jeschke, G., Mitchell, S., Perez-Ramirez, J. *Design of Flame-Made ZnZrO_x Catalysts for Sustainable Methanol Synthesis from CO₂* [Adv. Energy Materials, 13, 4, 2204122, 2023](#)
3. Asselman, K., Kirschhock, C., Breynaert, E. *Illuminating the Black Box: A Perspective on Zeolite Crystallization in Inorganic Media* [Acc. Chem. res., 56, 18, 2391-2402, 2023](#)
4. Bakken, K., Grendal, O.G., Einarsrud, MA. *In situ characterisation for studying nucleation and growth of nanostructured materials and thin films during liquid-based synthesis* [J Sol-Gel Sci Technol, 105, 596-605, 2023](#)
5. Baumgärtner, J.F., Wörle, M., Guntlin, C.P., Krumeich, F., Siegrist, S., Vogt, V., Stoian, D.C., Chernyshov, D., van Beek, W., Kravchyk, K.V., Kovalenko, M.V. *Pyrochlore-Type Iron Hydroxy Fluorides as Low-Cost Lithium-Ion Cathode Materials for Stationary Energy Storage* [Adv. Mater., 35, 49, 2304158, 2023](#)
6. Cerny, R., Brighi, M., Wu, H., Zhou, W., Dimitrievska, M., Murgia, F., Gulino, V., de Jongh, P.E., Trumpf, B.A., Udovic, T.J. *Thermal Polymorphism in CsCB₁₁H₁₂* [Molecules, 28, 2296, 2023](#)
7. Chen, Z., Zimmerli, N.K., Zubair, M., Yakimov, A.V., Björgvinsdóttir, S., Alaniva, N., Willinger, E., Barnes, A.B., Bedford, N.M., Copéret, C., Florian, P., Abdala, P.M., Fedorov, A., Müller, C.R. *Nature of GaO_x Shells Grown on Silica by Atomic Layer Deposition* [Chem. Mater., 35, 18, 7475-7490, 2023](#)
8. Da Costa, K.S., Summa, P., Gopakumar, J., van Valen, Y., Da Costa, P., Ronning, M. *Excess-Methane CO₂ Reforming over Reduced KIT-6-Ni-Y Mesoporous Silicas Monitored by In Situ XAS-XRD* [Energy Fuels, 37, 23, 18952-18967, 2023](#)
9. Danmo, F.H., Nylund, I.-E., Westermoen, A., Marshall, K.P., Stoian, D., Grande, T., Glaum, J., Selbach, S.M. *Oxidation Kinetics of Nanocrystalline Hexagonal RMn_{1-x}Ti_xO₃ (R = Ho, Dy)* [ACS Appl. Mater. Interfaces, Advanced Article, 2023](#)
10. Eggert, B.G.F., Belo, J.F.H., Araujo, J.P., Hauback, B.C., Frommen, C. *Structural transitions and magnetocaloric properties of low-cost MnNiSi-based intermetallics* [Intermetallics, 154, 107823, 2023](#)
11. Fatermans, J., Romolini, G., Altantzis, T., Hofkens, J., Roeyfaers, M.B.J., Bals, S., Van Aert, S. *Correction: atomic-scale detection of individual lead clusters confined in Linde type A zeolites* [Nanoscale, 15, 2436-2436, 2023](#)
12. Gelpi, M., García-Ben, J., Rodríguez-Hermida, S., López-Beceiro, J., Artiaga, R., Baaliña, A., Romero-Gómez, M., Romero-Gómez, J., Zaragoza, S., Salgado-Beceiro, J., Walker, J., McMonagle, C.J., Castro-García, S., Sánchez-Andújar, M., Señarís-Rodríguez, M.A., Bermúdez-García, J.M. *Empowering CO₂ Eco-Refrigeration With Colossal Breathing-Caloric-Like Effects in MOF-508b* [Adv. Mater., 2310499, 2023](#)
13. Golub, I.E., Heere, M., Gounaris, V., Li, X., Steenhaut, T., Wang, J., Robeyns, K., Li, H.-W., Dovgaliuk, I., Ikeda, K., Hautier, G., Filinchuk, Y. *Structural insight into the magnesium borohydride – ethylenediamine solid-state Mg-ion electrolyte system* [Dalton Trans., 52, 2404-2411, 2023](#)
14. Gopakumar, J., Benum, P.M., Svenum, I.-H., Enger, B.C., Waller, D., Ronning, M. *Redox transformations of Ru catalyst during NO oxidation at industrial nitric acid production conditions* [Chem. Engineering J., 475, 146406, 2023](#)

15. Gopakumar, J., Vold, S., Enger, B.C., Waller, D., Vullum, P.E., Ronning, M. *Catalytic oxidation of NO to NO₂ for industrial nitric acid production using Ag-promoted MnO₂/ZrO₂ catalysts* [Catal. Sci. Technol., 13, 2783-2793, 2023](#)
16. Grzechnik, A., Petříček, V., Chernyshov, D., McMonagle, C., Geise, T., Shahed, H., & Friese, K. *Incommensurate structures and radiation damage in Rb₂V₃O₈ and K₂V₃O₈ mixed-valence vanadate fresnoites* [Acta Cryst., B79, 2023](#)
17. Guerrero-Perez, M.O., Lapina, O.B., Rasmussen, S.B., Banares, M.A. *Combined Operando XANES and NMR and ESR Spectroscopies for the Determination of VPO Dynamic States* [Top. Catal., 66, 1161-1170, 2023](#)
18. Guesnay, Q., McMonagle, C.J., Chernyshov, D., Zia, W., Wieczorek, A., Siol, S., Saliba, M., Ballif, C., Wolff, C.M. *Substoichiometric Mixing of Metal Halide Powders and Their Single-Source Evaporation for Perovskite Photovoltaics* [ACS Photonics, 10, 9, 3087-3094, 2023](#)
19. Hamdalla, T.A., Aboraia, A.M., Shapovalov, V.V. *et al.* *Synchrotron-based operando X-ray diffraction and X-ray absorption spectroscopy study of LiCo_{0.5}Fe_{0.5}PO₄ mixed d-metal olivine cathode* [Sci. Rep., 13, 2169, 2023](#)
20. Hassen, S., Arfaoui, Y., Steenhaut, T., Filinchuk, Y., Klein, A., Chebbi, H. *A cationic Co(II) coordination polymer ¹⁻[Co(μ-L)(μ-Cl)(H₂O)₂]⁺ with the 4-amino-4H-1,2,4-triazole ligand: Structure, thermal behavior, and antimicrobial activity* [Inorg. Chimica Acta, 557, 121664, 2023](#)
21. Hua, W., Schweigart, P., Nylund, Lian, C., Cova, F.H., Svensson, A.M., Blanco, M.V. *Unraveling Effects of Current Density and Silicon on Silicon-Graphite Composite Anodes By in-Situ Synchrotron X-Ray Diffraction* [ECS Meeting Abstracts, MA2023-02, 315, 2023](#)
22. Hunvik, K.W.B., Seljelid, K.K., Wallacher, D., Kirch, A., Cavalcanti, L.P., Loch, P., Roren, P.M., Michels-Brito, P.H., Droppa-Jr, R., Knudsen, K.D., Miranda, C.R., Breu, J., Fossum, J.O. *Intercalation of CO₂ Selected by Type of Interlayer Cation in Dried Synthetic Hectorite* [Langmuir, 39, 14, 4895-4903, 2023](#)
23. Kirsch, A., Bøjesen, E.D., Lefeld, N., Larsen, R., Mathiesen, J.K., Skjærvø, S.L., Pittkowski, R.K., Sheptyakov, D., Jensen, K.M.O. *High-Entropy Oxides in the Mullite-Type Structure* [Chem. Mater., 35, 20, 8664-8674, 2023](#)
24. Klag, L., Gaur, A., Stehle, M., Weber, S., Sheppard, T.L., Grundwaldt, J.-D. *Role of Iron and Cobalt in 4-Component Bi–Mo–Co–Fe–O Catalysts for Selective Isobutene Oxidation Using Complementary Operando Techniques* [ACS Catal., 13, 21, 14241-14256, 2023](#)
25. Klimova, N.B., Snigirev, A.A. *Determining the Orientation of a Single-Crystal and the Absolute Energy of X-Rays Using Diffraction Losses* [J. Surf. Investig. 17, 1094–110, 2023](#)
26. Kochetygov, I., Roth, J., Pache, S., Espin, J., Schertenlieb, T., Justin, A., Taheri, N., Chernyshov, D., Queen, W.L. *A simple, transition metal catalyst-free method for the design of complex organic building blocks used to construct porous metal-organic frameworks* [Ang. Chem. Int., e202215595, 2023](#)
27. Korshunov, A., Hu, H., Subires, D., Calugaru, D., Feng, X., Rajapitamahuni, A., Yi, C., Roychowdhury, S., Vergniory, M.G., Stremper, J., Shekhar, C., Vescovo, E., Chernyshov, D., Said, A.H., Bosak, A., Felser, C., Bernevig, B.A., Blanco-Canosa, S. *Softening of a flat phonon mode in the kagome ScV₆Sn₆* [Nat Commun 14, 6646, 2023](#)
28. Kvande, K., Garetto, B., Deplano, G., Signorile, M., Solemsli, B.G., Prodingler, S., Olsbye, U., Beato, P., Bordiga, S., Svelle, S., Borfecchia, E. *Understanding C–H activation in light alkanes over Cu-MOR zeolites by coupling advanced spectroscopy and temperature-programmed reduction experiments* [Chem. Sci., 14, 9704-9723, 2023](#)
29. Lätsch, L., Kaul, C.J., Yakimov, A.V., Müller, I.B., Hassan, A., Perrone, B., Aghazada, S., Berkson, Z.J., de Baerdemaeker, T., Parvulescu, A.-N., Seidel, K., Teles, J.H., Copéret, C. *NMR Signatures and Electronic Structure of Ti Sites in Titanosilicalite-1 from Solid-State ^{47/49}Ti NMR Spectroscopy* [J. Am. Chem. Soc., 145, 28, 15018-15023, 2023](#)

30. Li, X., Yan, Y., Jensen, T.R., Filinchuk, Y., Dovgaliuk, I., Chernyshov, D., He, L., Li, Y., Li, H.-W. *Magnesium borohydride $Mg(BH_4)_2$ for energy applications: A review* [J. Materials Sci. and Technol., 161, 170-179, 2023](#)
31. Li, Y., Wu, Z. *A review of in situ/operando studies of heterogeneous catalytic hydrogenation of CO_2 to methanol* [Catal. Today, 420, 114029, 2023](#)
32. Liu, Q., Miao, Y., Villalobos, L.F., Li, S., Chi, H.-Y., Chen, C., Vahdat M.T., Song, S., Babu, D.J., Hao, J., Han, Y., Tsapatsis, M., Agrawal, K.M. *Unit-cell-thick zeolitic imidazolate framework films for membrane application* [Nat. Mater., 22, 1387–1393, 2023](#)
33. Loughran, R.P., Hurley, T., Gladysiak, A., Chidambaram, A., Khivantsev, K., Walter, E.D., Graham, T.R., Reardon, P., Szanyi, J., Fast, D.B., Miller, Q.R.S., Park, A.-H.A., Stylianou, K.C. *CO_2 capture from wet flue gas using a water-stable and cost-effective metal-organic framework* [Cell Reports Physical Science, 4, 7, 101470, 2023](#)
34. Luongo, G., Bork, A. H., Abdala, P. M., Wu, Y. H., Kountoupi, E., Donat, F., Müller, C. R. *Activation in the Rate of Oxygen Release of SrO . $8CaO$. $2FeO_3\text{-}\delta$ Through Removal of Secondary Surface Species with Thermal Treatment in a CO_2 -Free Atmosphere* [J. Mater. Chem. A, 11, 6530-6542, 2023](#)
35. Ma, H., Zheng, X., Zhang, H., Ma, G., Zhang, W., Jiang, Z., Chen, D. *Atomic Cu-N-P-C Active Complex with Integrated Oxidation and Chlorination for Improved Ethylene Oxychlorination* [Adv. Sci., 10, 2205635, 2023](#)
36. Marshall, K.P., Emerich, H., McMonagle, C.J., Fuller, C.A., Dyadkin, V., Chernyshov, D., van Beek, W. *A new high temperature, high heating rate, low axial gradient capillary heater* [J. of Synchrotron Radiation, 30, 267-272, 2023](#)
37. Meroni, D., Cionti, C., Silvestrini, L., Gal, N., Cazzaniga, M., Ceotto, M., Buccella, G., Lo Presti, L., Cappelletti, G. *Oxygen vacancies in the Spotlight: On the engineering of intrinsic defects in highly defective TiO_2 photocatalysts* [J. of Photochem. and Photobiology A, 444, 114916, 2023](#)
38. Muscarella, L.A., Jöbsis, H.J., Baumgartner, B., Prins, T.P., Maaskant, D.N., Petukhov, A.V., Chernyshov, D., McMonagle, C.J., Hutter, E.M. *Which Ion Dominates the Temperature and Pressure Response of Halide Perovskites and Elpasolites?* [J. Phys. Chem. Lett., 14, 40, 9042-9051, 2023](#)
39. Okatenko, V., Loiudice, A., Newton, M.A., Stoian, D.C., Blokhina, A., Chen, A.N., Rossi, K., Buonsanti, R. *Alloying as a Strategy to Boost the Stability of Copper Nanocatalysts during the Electrochemical CO_2 Reduction Reaction* [J. Am. Chem. Soc., 145, 9, 5370-5383, 2023](#)
40. Pittkowski, R.K., Clausen, C.M., Chen, Q., Stoian, D.C., van Beek, W., Bucher, J., Welten, R.L., Schlegel, N., Mathiesen, J.K., Nielsen, T.M., Du, J., Rosenkranz, A.W., Bojesen, E.D., Rossmeisl, J., Jensen, K.M.O., Arenz, M. *The more the better: on the formation of single-phase high entropy alloy nanoparticles as catalysts for the oxygen reduction reaction* [EES. Catal., 1, 950-960, 2023](#)
41. Potter, M. E., Mediavilla Madrigal, S., Campbell, E., Allen, L. J., Vyas, U., Parry, S., García-Zaragoza, A., Martínez-Prieto, L. M., Oña-Burgos, P., Lützen, M., Damsgaard, C. D., Rodríguez-Castellón, E., Schiaroli, N., Fornasari, G., Benito, P., Beale, A. M. *A High Pressure Operando Spectroscopy Examination of Bimetal Interactions in 'Metal Efficient' Palladium/ In_2O_3 / Al_2O_3 Catalysts for CO_2 Hydrogenation* [Ang. Chem., 62 \(45\), e202312645, 2025](#)
42. Quintero-Castro, D.L., Nilsen, G.J., Meier-Kirchner, K., Benitez-Castro, A., Guenther, G., Sakakibara, T., Tokunaga, M., Agu, C., Mandal, I., Tsrilin, A.A. *One-dimensional magnetism in synthetic Pauflerite, β - $VOSO_4$* [Phys. Rev. Materials, 7, 045003, 2023](#)
43. Rahimi, S., Stievano, L., Dubau, L., Ioioiu, C., Lecarme, A., Alloin, F. *Single-Atomic Dispersion of Fe and Co Supported on Reduced Graphene Oxide for High-Performance Lithium–Sulfur Batteries* [ACS Appl. Mater. Interfaces, 15, 38, 44932-44941, 2023](#)
44. Redekop, E.A., Cordero-Lanzac, T., Salusso, D., Pokle, A., Oien-Odegaard, S., Sunding, M.F., Diplas, S., Negri, C., Borfecchia, E., Bordiga, S., Olsbye, U. *Zn Redistribution and Volatility in $ZnZrO_x$ Catalysts for CO_2 Hydrogenation* [Chem. Mater., 35, 24, 10434-10445, 2023](#)

45. Salusso, D., Grillo, G., Manzoli, M., Signorile, M., Zafeiratos, S., Barreau, M., Damin, A., Crocellà, V., Cravotto, G., Bordiga, S. *CeO₂ Frustrated Lewis Pairs Improving CO₂ and CH₃OH Conversion to Monomethylcarbonate* [ACS Appl. Mater. Interfaces, 15, 12, 15396-15408, 2023](#)
46. Sannes, J.A., Gonano, B., Fjellvag, O.S., Kumar, S., Nilsen, O., Valldor, M. *X-ray and Neutron Diffraction Studies of SrTe₂FeO₆Cl, an Oxide Chloride with Rare Anion Ordering* [Inorg. Chem., 62, 32, 13081-13088, 2023](#)
47. Saseendran, D.P.A., Fischer, J.W.A., Müller, L., Abbott, D.F., Mougél, V., Jeschke, G., Triana, C.A., Patzke, G.R. *Copper(ii) defect-cubane water oxidation electrocatalysts: from molecular tetramers to oxidic nanostructures* [Chem. Commu., 59, 5866-5869, 2023](#)
48. Segura Lecina, O., Newton, M. A., Green, P. B., Albertini, P. P., Leemans, J., Marshall, K. P., Stoian, D., Loiudice, A., Buonsanti, R. *Surface Chemistry Dictates the Enhancement of Luminescence and Stability of InP QDs upon c-ALD ZnO Hybrid Shell Growth* [JACS Au, 3 \(11\), 3066–3075](#)
49. Sexton, A., Kanters, M., Demchenko, H., Pacáková, B., Fossum, J.O., Balzano, L. and Knaapila, M. *Classifying Tensile Loading History of Continuous Carbon Fiber Composites Using X-Ray Scattering and Machine Learning* [Adv. Eng. Mater., 26, 2301415, 2023](#)
50. Shahed, H., Sharma, N., Angst, M., Voigt, J., Persson, J., Prakash, P., Törnroos, K.W., Chernyshov, D., Gildenast, H., Ohl, M., Saffarini, G., Grzechnik, A., Friese, K. *Structural insight into the cooperativity of spin crossover compounds* [Acta Cryst. B, 79, 5, 354-367, 2023](#)
51. Stare, K., Stare, J., Skapin, S.D., Spreitzer, M., Meden, A. *Structure Determination and Analysis of the Ceramic Material La_{0.987}Ti_{1.627}Nb_{3.307}O₁₃ by Synchrotron and Neutron Powder Diffraction and DFT Calculations* [Crystals, 13, 439, 2023](#)
52. Steele, J.A., Solano, E., Hardy, D., Dayton, D., Ladd, D., White, K., Chen, P., Hou, J., Huang, H., Ali Saha, R., Wang, L., Gao, F., Hofkens, J., Roeffaers, M.B.J., Chernyshov, D., Toney, M.F. *How to GIWAXS: Grazing Incidence Wide Angle X-Ray Scattering Applied to Metal Halide Perovskite Thin Films* [Adv. Energy Mater., 13, 27, 2300760, 2023](#)
53. Stoian, D.C., Sugiyama, T., Bansode, A., Medina, F., van Beek, W., Hasegawa, J.-Y., Nakayama, A., Urakawa, A. *Dimethyl carbonate synthesis from CO₂ and methanol over CeO₂: elucidating the surface intermediates and oxygen vacancy-assisted reaction mechanism* [Chem. Sci., 14, 13908-13914, 2023](#)
54. Summa, P., Da Costa, K.S., Gopakumar, J., Samojeden, B., Motak, M., Ronning, M., van Beek, W., Da Costa, P. *Optimization of Co-Ni-Mg-Al mixed-oxides CO₂ methanation catalysts with solution combustion synthesis: On the importance of Co incorporation and basicity* [App. Mater. Today, 32, 101795, 2023](#)
55. Svitlyk, V., Kuz'min, M.D., Mozharivskiy, Y., Isnard, O. *Investigation of the intrinsic magnetic properties of GdCo₄B single crystal: determination of the magnetocrystalline anisotropy from the first-order magnetization processes* [Eur. Phys. J. Plus, 138, 388, 2023](#)
56. Thogersen, R.V., Fjellvag, A.S., Fjellvag, O. S., Fjellvag, H. *Structural and magnetic properties of antiferromagnetic-type Li_{5+x}Fe_{1-x}Co_xO₄* [J. of Inorganic and Gen. Chem., 649, 22, e202300146, 2023](#)
57. Ticali, P., Salusso, D., Airi, A., Morandi, S., Borfecchia, E., Ramirez, A., Cordero-Lanzac, T., Gascon, J., Olsbye, U., Joensen, F., Bordiga, S. *From lab to technical CO₂ hydrogenation catalysts: understanding PdZn decomposition* [ACS Appl. Mater. Interfaces, 15, 4, 5218-5228, 2023](#)
58. Tofoni, A., Tavani, F., Vandone, M., Braglia, L., Borfecchia, E., Ghigna, P., Stoian, D.C., Grell, T., Stolfi, S., Colombo, V., D'Angelo, P. *Full Spectroscopic Characterization of the Molecular Oxygen-Based Methane to Methanol Conversion over Open Fe(II) Sites in a Metal–Organic Framework* [J. Am. Chem. Soc., 145, 38, 21040-21052, 2023](#)
59. Werner, V., Aschauer, U., Redhammer, G.J., Schoiber, J., Zickler, G.A., Pokrant, S. *Synthesis and Structure of the Double-Layered Sillén–Aurivillius Perovskite Oxychloride La_{2.1}Bi_{2.9}Ti₂O₁₁Cl as a Potential Photocatalyst for Stable Visible Light Solar Water Splitting* [Inorg. Chem., 62, 17, 6649-6660, 2023](#)

60. Wieser, J., Knorpp, A.J., Stoian, D.C., Rzepka, P., Newton, M.A., van Bokhoven, J.A. *Assessing the Productivity of the Direct Conversion of Methane-to-Methanol over Copper-Exchanged Zeolite Omega (MAZ) via Oxygen Looping* [Ang. Chemie, e202305140, 2023](#)
61. Yartys, V.A., Berezovets, V.V., Vajeeston, P., Akselrud, L.G., Antonov, V., Fedotov, V., Klenner, S., Pöttgen, R., Chernyshov, D., Heere, M., Senyshyn, A., Denys, R.V., Havela, L. *Hydrogen induced structural phase transformation in ScNiSn-based intermetallic hydride characterized by experimental and computational studies* [Acta Materialia, 244, 118549, 2023](#)
62. Zhang, H., Dubey, R., Inniger, M., Okur, F., Wullich, R., Parrilli, A., Karabay, D.T., Neels, A., Kravchyk, K.V., Kovalenko, M.V. *Ultrafast-sintered self-standing LLZO membranes for high energy density lithium-garnet solid-state batteries* [Cell reports Physical Science 4, 101473, 2023](#)
63. Zhang, H., Okur, F., Cancellieri, C., Jeurgens, L.P.H., Parrilli, A., Karabay, D.T., Nesvadba, M., Hwang, S., Neels, A., Kovalenko, M.V., Kravchyk, K.V. *Bilayer Dense-Porous Li₇La₃Zr₂O₁₂ Membranes for High-Performance Li-Garnet Solid-State Batteries* [Adv. Sci., 2205821, 2023](#)
64. Zhang, H., Paggiaro, G., Okur, F., Huwiler, J., Cancellieri, C., Jeurgens, L.P.H., Chernyshov, D., van Beek, W., Kovalenko, M.V., Kravchyk, K.V. *On High-Temperature Thermal Cleaning of Li₇La₃Zr₂O₁₂ Solid-State Electrolytes* [ACS Appl. Energy Mater., 6, 13, 6972-6980, 2023](#)
65. Zhang, T., Steenhaut, T., Devillers, M., Filinchuk, Y. *Release of Pure H₂ from Na[BH₃(CH₃NH)BH₂(CH₃NH)BH₃] by Introduction of Methyl Substituents* [Inorganics, 11, 202, 2023](#)
66. Zhang, W., Ma, H., Wang, Y., Regli, S.K., Ronning, M., Rout, K.R., Margossian, T., Chen, D. *In situ monitoring of dynamic behavior of La-doped CuCl₂/γ-Al₂O₃ catalyst in ethylene oxychlorination* [J. of Catalysis, 417, 314-322, 2023](#)
67. Zhou, W., Docherty, S.R., Ehinger, C., Zhou, X., Copéret, C. *The promotional role of Mn in CO₂ hydrogenation over Rh-based catalysts from a surface organometallic chemistry approach* [Chem. Sci., 14, 5379-5385, 2023](#)